62-3-1

PROGRESS REPORT NO. 2

ON

INFLUENCE OF LUBRICATION ON ENDURANCE OF ROLLING CONTACTS

PERIOD September 22, 1961, to February 22, 1962

Submitted to:

U.S. DEPARTMENT OF THE NAVY

CHIEF, BUREAU OF NAVAL WEAPONS

WASHINGTON 25, D.C.

N. E. Sindlinger

J. A. Martin

D. F. Huttenlocher

U.S. Navy Contract No. NOw-61-0716-C
U.S. Navy Control No. 4658-61
SKF Report AL62T004
SKF Code 6402 1356
SKF Project III-1
SKF Reg. 414 2

RESEARCH LABORATORY
SKF INDUSTRIES, INC.
PHILADELPHIA, PA.

PROGRESS REPORT NO. 2

ON
INFLUENCE OF LUBRICATION ON ENDURANCE
OF ROLLING CONTACTS

PERIOD September 22, 1961, to February 22, 1962

Submitted to:

U.S. DEPARTMENT OF THE NAVY
CHIEF, BUREAU OF NAVAL WEAPONS
WASHINGTON 25, D.C.

Reported:
H. E. Sindlinger
J. A. Martin
D. F. Huttenlocher

Supervised:
T. A. Gilfillan

Approved:
Robert Fallon

U.S. Navy Contract No. NOw-61-0716-C
U.S. Navy Control No. 4658-61
SKF Report AL62T004
SKF Code 6402 1356
SKF Project III-1
SKF Reg. 414 2

RESEARCH LABORATORY
SKF INDUSTRIES, INC.
PHILADELPHIA, PA.

TABLE OF CONTENTS

LIST OF ENCLOSURES

PROGRESS REPORT NO. 2

INFLUENCE OF LUBRICATION ON ENDURANCE OF ROLLING CONTACTS

SUMMARY:

This report is the second progress report in a comprehensive experimental and theoretical study of lubrication effects on the endurance of rolling contacts under Contract NOw-61-0716-C.

The experimental studies on this program involve three basic types of machines: the Rolling Four-Ball Tester of the type similar to that used by Barwell (1)*, a Flat Washer and Rolling Element machine of the type used by SKF Industries, Inc., and a Two-Ball Apparatus being developed especially for this investigation. In the four-ball and two-ball machines the contact conditions and lubrication between two balls in rolling contact, both with and without different kinds and degrees of slip, can be studied. Flat washer testing of other element configurations will be conducted as the program progresses.

Elastohydrodynamic lubrication theory for the generation of lubricant film pressures between two rollers or balls has been reviewed. Recent developments reported in the literature are presented for use in calculating theoretical lubrication parameters in practical experimental systems. The development of a new electrical conductivity technique for the study of the lubricant and contact conditions in the rolling four-ball tester is described, and some contact lubrication effects detected in preliminary experiments with this new technique are presented. Radioisotope tracer tests to detect metal transfer under different lubrication conditions in the four-ball machine are in the final preparatory stages. They are intended for correlation with the conductivity studies.

All the above studies are aimed both at defining the limits of full-film elastohydrodynamic lubrication and at a study of contact lubrication in the elastohydrodynamic and boundary regimes.

---

*Numbers in parentheses refer to references at the end of this report.

A bank of four-ball machines are being readied for endurance testing under lubrication conditions defined by the above mentioned techniques. Well defined, high purity test lubricants have been selected to represent a cross-section of lubricant fluids. A basic understanding of elastohydrodynamic effects on endurance, of course, will require precise measurements of the temperatures and pressures or deflections at rolling contacts in order to relate these lubrication parameters to bearing failure processes. Such studies will be undertaken later with the two-ball machine, designed to allow precise measurement of the deflections and lubricant film thickness between two rolling balls using refined X-ray techniques based on the X-ray film-thickness method developed previously (2).

The recent progress and results in the above research efforts are presented in the following sections.

ELASTOHYDRODYNAMIC LUBRICATION THEORY

Since Reynolds first applied the Navier-Stokes equation for the behavior of viscous fluids to the problem of the lubricant flow in films between bearing surfaces (3), the resulting hydrodynamic lubrication theories have found extensive use in design and performance calculations for plain bearings. This success of hydrodynamics in providing a theoretical basis for lubrication problems, of course, led to the early development of hydrodynamic lubrication theories for rolling contacts (4). However, these early theorists assumed that the bearing surfaces were perfectly rigid and that the lubricant viscosity was constant, as it can reasonably be assumed for plain bearings. This resulted in the prediction of lubricant film thicknesses at rolling contacts of the same order of magnitude as the atomic spacings in the bearing metal, for conditions under which many bearings and gears were known to operate successfully. This fact, together with the mathematical complexity of any real improvements on the above assumptions, resulted in the wide-spread belief that the generation of hydrodynamic lubricant films at rolling contacts was not possible and that lubrication problems for such systems could only be solved by thin-film or boundary methods to be studied on the molecular scale.

On the other hand, the design of rolling bearings has been based almost entirely on the contact theory of Hertz (5) assuming static, frictionless surfaces. On this basis, and assuming "adequate lubrication", highly successful empirically based methods were evolved for prediction of bearing fatigue life (6). Bearing catalog life ratings based on these theories do not distinguish lubricant effects. It has been found in many recent studies, however, that lubricants indeed have a profound effect on bearing endurance (7-13). In addition, recent developments in measurement techniques (14-16) have shown that the lubricant films at rolling contacts, even though very thin, are nevertheless much thicker than molecular dimensions. Such new evidence, together with the development of new mathematical techniques and high speed digital computors, has inspired considerable recent development of elastohydrodynamic theory, in which the equations of elasticity theory for the elastic deformation of the bearing surfaces are solved simultaneously with hydrodynamic equations for the flow of the lubricant, considering an exponential increase in viscosity with pressure.

1-1 Theories for "Line" Contact

Lubrication theories are most easily developed for the infinitely wide bearing, which in the case of rolling bearings, is the so-called "line" contact as between two cylindrical rollers without end effects. Most elastohydrodynamic theory is for "line" contacts, as discussed in Progress Report No. 1 on this program. Some of these theories can be applied qualitatively to the lubrication of balls in the present program, and since the "line" contact theories have been more extensively developed than the "point" contact theories, the mathematical techniques used should be studied for eventual application to the three-dimensional problem.

Theory by Dowson and Higginson. Dowson and Higginson (17) solved the "line" contact elastohydrodynamic problem by a numerical technique. This technique involves the determination of a pressure distribution over the contact which produces compatible film shapes when both the elastic and the hydrodynamic requirements of the system are satisfied. They showed that the film shape required to yield a given pressure curve can be determined completely using hydrodynamic equations. The shape of the elastically deformed surface can also be determined from the assumed pressure curve and then be compared with the hydrodynamically obtained film shape.

Dowson and Higginson assume that, as the load is increased, the pressure distribution in the contact area approaches the Hertzian pressures, except in the inlet and outlet regions. This assumption is essentially the same as that used by Grubin (18), discussed in the previous report. To solve a specific elastohydrodynamic problem, a load is first selected and the corresponding Hertzian pressure distribution calculated. Then a trial pressure curve is chosen by modifying the Hertzian curve, and the film thickness is computed. The film shapes computed from hydrodynamic and elastic equations are then compared, and further trials made as necessary if too large a discrepancy occurs between the two curves. The solution of the elastohydrodynamic problem is considered obtained when the curves match each other within some specified tolerance.

The mathematical results obtained by Dowson and Higginson show a tendency of the contact pressure distribution toward Hertzian and of the film shape toward parallel as the load increases. They also support Cameron's speculation (19) that at high loads film

thickness would become insensitive to increase in load. Dowson and Higginson have evaluated a number of specific cases by the above method and have correlated these numerical results into a formula for minimum film thickness (20), as follows:

$$H = 1.6 \frac{G^{0.6} U^{0.7}}{W^{0.13}}$$

where

$$H = h_{mm}/R$$
$$G = \gamma E^*$$
$$U = \eta_0 u/(E^* R)$$
$$W = w/(E^* R)$$

and

h_{mm} = minimum film thickness

R = effective radius of a roller on a flat $\left(\frac{1}{R} = \frac{1}{R_1} + \frac{1}{R_2}\right)$

w = load per unit width of the contact

η_0 = absolute viscosity at atmospheric pressure and temperature

γ = pressure coefficient of viscosity

u = surface velocity of rollers

E^* = reduced Young's modulus defined by

$$\frac{1}{E^*} = \frac{1}{2}\left[\frac{1-\sigma_1^2}{E_1} + \frac{1-\sigma_2^2}{E_2}\right]$$

where $\sigma_{1,2}$ is Poisson's Ratio and $E_{1,2}$ is Young's modulus for the two contact bodies

Dowson and Higginson have also calculated some examples of the effect of elastohydrodynamic lubricant pressures on the subsurface stresses at rolling contacts (21). Enclosure 1 shows a few typical curves. The most notable result is that with certain loads, speeds, curvatures, and material properties, the Dowson and Higginson solution shows that a secondary maximum of shear stress is generated that can be higher than the Hertzian maximum.

Archard, Gair, and Hirst Theory. Archard, Gair, and Hirst (22) solved essentially the same elastohydrodynamic problem as Dowson and Higginson, above, and Poritsky, Petrusevich, and Grubin, discussed in Progress Report No. 1, using an iterative technique with a computor. They present the following principal results:

a) The hydrodynamic equations contain only the following independent dimensionless variables

Dimensionless pressure $\bar{P} = P\theta$, where θ is an elastic constant*

Dimensionless pressure-viscosity $\Lambda = \beta\theta$, where β is a pressure-viscosity coefficient

Dimensionless velocity $\bar{U} = \eta_0 \frac{U\theta}{R}$, where η_0 is the viscosity at atmospheric pressure

U is the sum of the surface velocities

R is half the harmonic mean of the curvature radii

Whenever two problems are identical in these variables, the film geometry will be identical in the variables

$H = \frac{h}{R}$ where h is the film thickness

$X = \frac{x}{R}$ where x is the length coordinate across the contact.

b) For an oil of 40 cp, and rollers of 1.5 in. diameter, numerical solutions were obtained for varying loads, speed, pressure viscosity and elastic constants.

---

* θ is defined as follows: $\theta = 2(1-\sigma^2)/\pi E$, where σ is Poisson's ratio and E is Young's modulus.

Fig. A in Enclosure 2 shows the film thickness h_o at the point of maximum pressure as a function of speed and load. It is stated that h_o varies approximately as the -1/4 power of the maximum Hertz stress P, as the 0.7 power of speed U, and inversely as the pressure-viscosity coefficient β. The effect of the elastic constant θ is negligible.

c) Pressure distributions as a function of velocity, load, and viscosity, are given graphically, Fig. B, Enc. 2 showing a typical distribution. Deviation from Hertzian distribution increases with speed, viscosity and elastic modulus, and with decreases of load and pressure-viscosity coefficient.

d) The Hertzian relationship between load and maximum surface pressure is disturbed very little. However, there is a typical high and sharp pressure peak in the outlet region, which, if experimentally confirmed, will cause a high secondary subsurface shear stress maximum. Corresponding to the pressure peak, there is a thinning of the film to about 75% of that prevailing in the Hertzian region.

Dörr Theory. As discussed in the first Progress Report, Dörr has developed what is probably the mathematically most satisfying elastohydrodynamic theory for an isoviscous lubricant (23). Recently, Dörr has been extending his theory for lubricants having an exponential variation of viscosity with pressure, using a much more extensive analytical approach than has hitherto been available (24). At the present time, final results of his work are not available.

Bell's Non-Newtonian Theory. In his most recent work Bell (25) has developed a theory for film thicknesses in rolling contact with a non-Newtonian fluid, as compared to the lubricants having Newtonian viscosity discussed in all of the above theories. Bell assumes that the lubricant behaves as a Ree-Eyring fluid in which shear stress τ and shear rate $\dot{s}$ are related by the following expression

$$\tau = \frac{X}{\alpha} \sinh^{-1}(\beta \dot{s})$$

where $\alpha = \alpha_0 e^{\gamma_1 p}$ & $\beta = \beta_0 e^{\gamma_2 p}$

and the quantities α, α_0, β_0, γ_1, and γ_2 are constants at a constant temperature, and p is pressure.

Bell makes the assumption that the film thickness in the contact area is constant and the contact area has the Hertzian form. He suggests that the film thickness developed in the contact zone is much dependent on the mechanical process occurring in the entering section. He further assumes that the shape of the film in the entering section can be taken as the deformed shape of the surfaces determined by Hertz theory outside the contact area, as follows:

$$h = (\eta_0 + f)\frac{P}{E'}$$

where P is the load applied per unit length, E' is a reduced Young's modulus*, and η_0 and f are defined as

$$\eta_0 = \frac{E' h_0}{P}$$

$$f = 2\xi\sqrt{\xi^2 - 1} - 2\ln\left(\xi + \sqrt{\xi^2 - 1}\right)$$

$$\xi = \frac{x}{x_h}$$

where x_h is the half width of the Hertz contact area.

The equations obtained are difficult to solve. Bell developes upper and lower bounds for the solution and then combines them to yield a final approximate equation for the film thickness h_0 which is valid for pure rolling.

The solution is presented as a graph shown as Figure C in Enclosure 2. In this figure the dimensionless parameter $1/\lambda$ is plotted as the ordinate against

$$\frac{\mu_0 \gamma V}{R}\left(\frac{P}{E'R}\right)^{-\frac{1}{8}}\left(\frac{4R}{\beta_0 V}\right)^{\frac{11}{8}}$$

---

*Bell's E' differs from Dowson and Higginson's E^* by a factor of $2/\pi$, such that $1/E' = 2/(\pi E^*)$.

as the abscissa, showing a family of curves with γ_2/γ_1 as the parameter. Here λ is defined as

$$\beta_o V/(4h_o)$$

where β_o = a lubricant property which is proportional to the relaxation time,

V = the sum of the surface velocities at the contact in the direction of rolling,

γ_1 and γ_2 = the pressure-viscosity coefficients of α and β, respectively,

$\gamma = \gamma_1 + \gamma_2$ = the ordinary pressure-viscosity coefficient,

μ_o = absolute viscosity at the environmental pressure and temperature,

R = half the harmonic mean of the radii of curvatures at the contact = $1/(1/R_1 + 1/R_2)$,

P = the load per unit width of the contact.

The Bell theory yields lower values for h_o than the Newtonian theories, as seen by comparison with the curve for the Newtonian theory by Grubin (18), also shown in Figure C of Enclosure 2. (Experimental values appear to fall between the Newtonian and the Bell values.) However, the Bell theory approaches the Newtonian theory at low values of λ, i.e. at low rolling speeds with lubricants having short relaxation times under conditions when the film thickness is fairly large.

Other Non-Newtonian Theories. In their recent work, Crouch and Cameron (26) have derived a lubrication theory using graphical methods in which the lubricant is assumed to conform to the Maxwell model (having visco-elastic properties) in which the viscosity varies with pressure. This theory is also extended to "point"

contacts between spheres. Milne (27) and Burton (28) have also developed rolling-contact lubrication theories using Maxwell lubricants, and Kotova (29) and Sasaki, et al (31) have used the Bingham model of a plastic body for the non-Newtonian behavior of the lubricant. The Sasaki theory is extended for complete roller bearings, as is the theory by Osterle (30) for isoviscous Newtonian lubricants. The details of these other theories will be reported later as the need arises.

Thermal Theories. The temperatures which exist in elastohydrodynamic films have been studied by Archard (32). Archard applied the flash temperature theory developed by Blok (33) and Jaeger (34). Using this theory, he derives the surface temperature in terms of the rate of heat supply, the size and speed of the heat source, and the thermal properties of the material. Next, Archard computes the temperature increase in the oil film above the surface temperature by considering steady state conditions and assuming a generation of heat uniformly distributed through the film and dissipation of the heat by conduction in the direction perpendicular to the surfaces. The rise in oil temperature on the median plane above the surface temperature is approximated by

$$\theta = \frac{h \mu w' (v_1 - v_2)}{16 J K_1 b}$$

where θ = rise in temperature above the surface temperature,

K_1 = thermal conductivity in the oil,

h = film thickness,

μ = the coefficient of friction,

w' = the normal load per unit contact width,

v_1 and v_2 = surface velocities,

J = the mechanical equivalent of heat,

b = the half-width of the contact area.

Archard finally examines the case where all heat is generated in the center plane of the film and finds that the oil film temperature rise computed in this manner is twice that obtained assuming uniform heat generation in the film. It is concluded from numerical comparison that the temperature rise within the oil film, under certain operating conditions, substantially exceeds the surface temperature rise above ambient. Archard's formula yields zero temperature rise in the film for pure rolling.

The rolling-contact therma. theory by Sternlicht, et al (35), assumes adiabatic conditions in the lubricant film as opposed to the predominant conduction processes predicted by other theorists (32, 17).

1-2 Theories for "Point" Contact

In the early theories for "point" contact, as distinguished from those for "line" contact discussed above, Howlett (36) and Kapitsa (37), whose theory was discussed in Progress Report No. 1, both assumed rigid ball surfaces.

Archard and Kirk (38) have developed a simplified theory of elastohydrodynamic lubrication for point contact by using the same basic hydrodynamic equation as Kapitsa used in his analysis of ball bearing lubrication theory. By setting up a criterion of maximum load carried equivalent to

$$P'_{MAX} = 1/\alpha$$

where P'_{max} is the maximum reduced pressure and α is the pressure-viscosity coefficient, they obtained a first approximate value h_1 of the thickness of the parallel film existing under elastohydrodynamic conditions

$$h_1 = 0.67 (\alpha \eta_0 v)^{\frac{2}{3}} R^{\frac{1}{3}}$$

which is similar to the equation of Kapitsa discussed in Progress Report No. 1.

A more complete analysis of elastohydrodynamic lubrication at "point" contacts was also made (but not fully published) by Archard and Kirk, using methods similar to those employed by

Grubin in his anslysis of "line" contacts. By taking into account the side leakage effect, the film thickness is obtained as

$$h_2 \cong 0.84(\alpha \eta_0 V)^{0.741} R^{0.407} (E/w)^{0.074}$$

where h_2 = film thickness in cm,

α = the pressure-viscosity coefficient in $cm^2/dyne$,

V = sum of the surface velocities in cm/sec,

η_0 = viscosity at atmospheric pressure in poise,

R = equivalent radius of a ball on a flat in cm = $1/(1/R_1 + 1/R_2)$,

E = modulus of elasticity in $dynes/cm^2$,

w = load in dynes.

1-3 Summary

The elastohydrodynamic theory of line contact appears well established for conditions of isothermal flow. The film thickness equation by Archard and Kirk can serve as a guide for point contact. Thermal and non-Newtonian theories are in their early stages. In the present work, theory will be used in two ways:

a) Calculations of film thickness and pressure distribution in the contact zone will be made for comparison with the experimental results.

b) Using experimental film thickness profiles, an analysis of contact stresses is planned.

In order to provide reliable methods for the latter purpose, SKF Industries has, using corporate funds, entered into a contract with Battelle Memorial Institute for a feasibility study on a numerical method for stress computation in ball contacts where the surface deformation topography is experimentally known.

CONDUCTIVITY TECHNIQUES FOR THE DETECTION OF LUBRICANT FILMS

Conductivity testing, with a rolling four-ball test machine, has been conducted at SKF Industries, in order to attain a better understanding of contact phenomena with lubricated, rolling balls. The initial conductivity test program has covered a study of operational parameters such as load, speed, viscosity, and surface finish, regarding their effects on producing separation of the contact surfaces with a lubricating film. Although an extensive program of testing and analysis, both with the four-ball tester and other test apparatus, will be required to more fully understand the relationship between data obtained by electrical methods and lubrication phenomena at rolling contacts, the test data now available make it possible to draw certain conclusions, and have established feasibility of the method.

2-1 Equipment Description and Test Conditions

The rolling four-ball configuration has been previously shown on Enclosures 11 and 12 of Appendix I to Progress Report No. I. Basically, the test method consists of introducing an electrical potential difference between the upper driving ball and one or more of the three lower driven balls, and interpreting voltage measurements obtained across the contact, in terms of separation between the rolling elements.

Development of Electrical Circuitry. Initial conductivity testing was attempted with an arrangement similar to that shown on Enclosure 15(a) of Progress Report No. I. The shorting contacts, in this instance, consisted of a bronze, rifle cleaning brush. Testing with this brush was discontinued when it was discovered that the bristles tore loose from their holder and entered the rolling contact region.

The four-ball test configuration now being utilized is shown on Enclosure 3 . The top ball is adhesive bonded to the driving spindle to avoid shifting of the ball axis. Two electrical contactors are mounted in the rotating plastic cage so that they bear against one of the lower test balls. Three mercury slip ring assemblies are utilized to make electrical connections to the rotating

elements. The circuit runs from the ground through the upper slip ring into the spindle and upper ball, across the upper and lower test balls (when in contact), through the lower test ball into one of the electrical contactors, and out one of the lower slip rings to the voltage source (other terminal of source grounded). The second contactor on the lower ball, and its associated slip ring, are used for periodic monitoring of the contactors.

The contactors used are known as "fuzz buttons", which is the tradename for wound copper alloy wire contactors produced by Technical Wire Products, Inc., Springfield, New Jersey. The contactor is formed from a single wire, which greatly reduces the likelihood that loose pieces of wire will enter the contact area. The particular contactors used are gold plated copper alloys of 97% copper and 3% silver. Enclosure 4 shows microphotographs of one of the 0.188" diameter contactors.

To ascertain their contact properties, a test was conducted with "fuzz buttons" in contact with the equator of a ball which was adhesive bonded to a spindle rotating at 400 rev./min. With an applied voltage of 100 millivolts across the two contactors, the voltage drop across the contacts in a 50 kΩ circuit was measured to be no more than 10 microvolts. The test was discontinued after four hours running time when no increase in the voltage was observed. The performance of the contactors was also monitored on an oscilloscope where it was shown that a steady signal was obtained for the duration of the test. It was noticed, however, that a minimum contact pressure was necessary in order to assure proper contact with the lubricated ball. In future testing the contactor will be spring loaded against the ball at a point as near the pole of rotation as possible, so that relative rotation effects are minimized. For the testing that was conducted during this reporting period the contactors were compressed in holes in the cage, and the elasticity of the contactor itself was utilized to provide the spring pressure.

Mercury slip rings have been retained for this series of tests, to avoid the complication of additional experimentation with solid slip rings until the conductivity testing has been proven out. The use of solid slip rings is planned in the future because it will greatly simplify assembly and disassembly of the rig and will make it possible to operate at high speeds (small diameters will be used).

The electrical circuit now being utilized is shown on Enclosure 5 . As shown, the contact is in series with a 56 kΩ resistor, and the contact circuit receives a DC voltage from a 3 kΩ voltage divider across a 1.5 v dry cell. This arrangement makes it possible to adjust the open contact voltage level to 100 mv, which is the voltage level used in all of the test series so far conducted. The 56 kΩ series resistor limits the current through the contact to a maximum of 2 μa. The switch provided in series with the contacts simulates an open contact, and is utilized for voltage calibration purposes.

The sensing circuits are connected in parallel across the contact and consist of a Cathode Ray Oscilloscope, a Vacuum Tube Voltmeter and a DC Amplifier. A dual beam oscilloscope is utilized for monitoring both the input and output signal of the amplifier. Switching is provided so that the voltmeter may monitor either the input or output of the amplifier. The amplifier is used to feed a scaler (electronic counter with a built-in time base) having a voltage level discriminator such that a count is registered each time the input voltage crosses upwards over the preset discriminator voltage. By comparing voltmeter readings across the amplifier input and output, with the calibration switch open, the amplification may be determined and the discriminator setting may be referenced back to the input circuit.

By inserting a 10 kc square wave into the input circuit, the frequency response of the total circuitry was estimated. Observations of the oscilloscope showed rise times of approximately 2.0 microseconds, which suggests a flat response up to approximately 50 kc (the DC amplifier is only guaranteed a flat response up to about 15 kc, but apparently is adequate beyond that limit).

Equipment Check Out. A check was made of the machine vibration level by mounting accelerometers on the cup housing and running tests with varying combinations of load and speed. The maximum acceleration obtained was about 0.15 g's. The spring supported mass attached to the cup weighs 21 lbs. Taking into account the contact angle of the bearing configuration, and neglecting the vibration mount restraining force, vibratory forces of about 4 lbs. result. These are considered negligible in comparison with the applied loads.

A plastic enclosure is used to cover the rolling elements and slip ring assemblies to aid in excluding dirt and moisture. Dry nitrogen blanketing is utilized both in the oil reservoir and plastic enclosure to further maintain a dry atmosphere. The entire system is thoroughly flushed with naphtha which is allowed to evaporate before the test oil is introduced and testing is commenced.

A problem inherent in the four-ball configuration is that alternate routes of current can exist with a metallic cup. If the cup is grounded, it may be seen from the circuit diagram shown in Enclosure 5 that current may flow not only from the lower ball (with the electric contactors) to the top ball, but also from the lower ball to the cup. A direct short could then be indicated even though there might be separation between the upper and lower balls.

If the cup is isolated (floating), a second route of current flow is possible from one lower ball to the cup through another lower ball, and then to the upper ball. This route of current flow can, of course, only occur if there is no film between two lower balls and the cup at the same time.

In most instances, it was found that a continuous film was not developed between the lower balls and the cup, so that it was generally necessary to have a floating cup with respect to ground potential. Under light load conditions, however, a test was successfully conducted wherein the cup was grounded with no apparent effects on readout.

A second test was then conducted in which the cup was brought up to 100 mv potential above ground by means of a second battery and voltage divider. This secondary circuit is shown in dashed lines on Enclosure 5. In this instance the lower ball (with electrical contactor) will always be at full potential whether the lower ball and cup are in contact or not. It will only be at ground potential when the lower ball contacts the upper ball. In this arrangement, no erroneous indications will occur from alternate paths of current. More frequent contact should be shown when the cup is grounded than when the cup is at full potential, if there is significant lower ball to cup contact. In the one comparative test conducted, there was no noticeable difference whether the cup was grounded, floating, or at 100 mv. It may be assumed that in this test a full film existed between the lower balls and cups.

In all test series reported below, the cup floated. Possible difficulties from hum pickup were overcome by shielding. Effects of second routes of current are believed to be small.

Further testing is planned to evaluate ball to cup separation over the entire load, speed, lubricant range. Depending on results, the cup will be operated grounded, at 100 mv, or isolated, whichever yields best operation and freedom from secondary current routes.

It has been determined that the original cup surface finish was about 10 microinches rms, and that after extensive running the surface finish was improved to about 4 microinches rms. The rougher surface finish of the cup as compared to the ball, may account for the fact that full films were not established under all conditions between the balls and cup well in advance of the establishment of a full film between the upper and lower ball, even though the unit pressures are much lower for the ball to cup contact than for the ball to ball contact.

The test arrangement described so far was used in obtaining data in the final test series to be analyzed further below. Prior to arriving at the test arrangements which have been described, it had been found necessary to make modifications to some parts of the test apparatus and electrical circuit. Tests had been attempted with a top ball which was not bonded to the driving spindle. It was found that this caused erratic results in ball tracking as the ball would shift its axis. Reasonably high loads (150 lbs.) are required before the upper ball will maintain a fixed axis if unbonded. A transformer had been used in lieu of the DC amplifier and this resulted in rather poor definition of the signal submitted to the electronic counter. The atmosphere surrounding the test elements and oil reservoir had not been controlled with respect to humidity and cleanliness. The exact effects of testing in an uncontrolled atmosphere are difficult to define, but it certainly adds an unnecessary variable. Finally, an electronic counter was originally utilized which had poor discriminator setting control, and resulted in uncertainties regarding the level at which counts were obtained. Preliminary test data were obtained during development of the test arrangement and are contained in Enclosures 10 - 12 (which will be discussed in more detail later). These preliminary data should be regarded as indicating trends only.

2-2 Test Lubricants

The lubricants used are described in detail in section 4 of this report. Two test oils were utilized for the final series of tests conducted with the modified test apparatus. These oils were obtained from Esso and are designated as Esso Primol 355 with a viscosity of 75 centistokes at 100°F, and a special limited quantity sample oil with a MLO-7588 base with a viscosity of 23.2 centistokes at 100°F. These oils are both highly refined mineral oils containing no additives other than traces of oxidation inhibitors. The oils were dried to remove any moisture, and were filtered through one-half micron Millipore filters.

The preliminary test series lubricants are also described in detail in section 4 of this report, and are a white pharmaceutical mineral oil (80 centistokes at 100°F), a polyolefin lubricant with a mild EP additive (MLO-7584, 117 centistokes at 100°F), and a diester base lubricant (MLO-7593, 24 centistokes at 100°F).

2-3 Test Data

Final test series results obtained with the final test setup are now given as follows:

Enclosure 13 shows maximum Hertz stress as a function of load applied to the upper ball.

Enclosure 6 shows curves of voltmeter reading across the contact as a function of speed with load as a parameter, for Esso Primol 355 lubricant. The voltage readings are generally steady, due to the averaging performed by the voltmeter time constant. It is seen from the curves that the voltage increases steadily with speed for any given load and reaches the 100 millivolt value corresponding to zero current across the contact at speeds depending on the load. The curves shift from left to right in a consistent manner as the load is increased. The curves appear to have a characteristic shape, concave from above for low voltages and convex for high voltages.

In Enclosure 7 a repeat of the same test is shown using the same balls as in Enclosure 6. The curves are similar in appearance; however, the curve for any given load in Enclosure 7 falls to the left of the corresponding curve on Enclosure 6. This will become understandable when the effect of running-in and plastic deformation of the balls will be discussed.

Enclosure 8 shows the number of counts (interruptions of contact voltage) per rolling cycle* for the test for which the average voltages were shown in Enclosure 6, and Enclosure 9 shows the same counts corresponding to the repeat test for which the average voltages were shown in Enclosure 7.

The count rate curves were obtained with a discriminator setting corresponding to 50 millivolts across the contact. It is seen that for speeds where voltage measurements are just obtainable that the count rate is very near a maximum value. In future testing test points will be obtained to determine the slope of the curve for lower speeds than those shown. Beyond the maximum value the count rate rapidly decreases, and then gradually tapers off again, to become practically zero for speeds at which the voltage across the contact is equal to 100 millivolts. Count rates for the repeat test, Enclosure 9, correspond to the voltage measurements for the same test, i.e. the curves fall to the left of those for the first test series.

Photographs were not taken of oscilloscope traces during the final test series. However, the oscilloscope patterns were identical to the eye with those obtained in the preliminary test series, and, therefore, reference is made to Enclosure 14 showing oscilloscope traces taken at the preliminary test series. Fig. A shows a typical trace obtained when the contact voltage measured was low. Fig. B is a trace obtained when the contact voltage was approximately 50 millivolts.

Fig. C was taken with a voltage close to 100 millivolts. Fig. D is taken at a condition similar to Fig. B except with a much faster sweep rate.

It is seen that the oscilloscope trace does not always alternate between zero and 100 millivolts but there are peaks at many voltage levels, predominately low levels in Case A, predominately high levels in Case C, and all levels between zero and 100 millivolts in Case B. The fast sweep trace in Fig. D shows the voltage holding at an intermediate level for a finite period of time.

---

*A rolling cycle is the time elapsed between two successive passages of a given lower ball over a fixed point on the upper ball.

Tests were also attempted with the special Esso oil (MLO-7588 base). Enclosure 15 shows the results of a break-in test with this oil (break-in tests will be discussed later). Following a considerable amount of running time, only a relatively low voltage level was obtainable. Further tests were conducted at higher operating speeds which showed only a small gain in the average voltage level. The speed for the test apparatus is limited by the mercury slip rings, so that conclusive data could not be obtained. It was also apparent that the voltage readings were quite unstable, since the voltage would fluctuate as much as 20 millivolts with constant test conditions. Further testing with this oil was discontinued for this reporting period.

Preliminary Test Series. The preliminary test data curves of average contact voltage as a function of speed, with load as the parameter, are shown on Enclosures 10-12 for general reference only. It may be seen by comparing these curves with those of Enclosures 6 and 7 that the same characteristic behavior, which has been discussed, is evident.

Enclosure 10 shows voltage measurements with a white mineral oil. With the exception of the curve for 25 lbs. and the last point on the curve for 75 lbs. the data shows that the initial point where voltage readings are obtainable is only slightly affected by load, that there is a relatively sharp rise in voltage to about 70 to 90 millivolts, and that the slope decreases with increasing load. Enclosure 12 shows voltage measurements for a Diester lubricant. With the exception of the curve for a 75 lb. load, the curves show that the slope of the voltage curves increase slowly with a speed increase, and that increasing load increments appear to have more effect than with the mineral oil. The speed was cut-off at 384 rev. per min. as a low speed gear box was being utilized at the time. Enclosure 11 shows voltage measurements for a Polyolefin lubricant. A very similar set of curves is obtained in this case, however, quite erratic behavior is exhibited in that the best separation is shown for the highest load. The curves do exhibit the same characteristics as the curves previously described.

The curves of count rates have not been presented for the preliminary tests in view of their extremely erratic behavior, and the fact that the transformer and particular electronic counter employed were later found to produce unreliable results.

Break-in of New Balls. In all testing, it has been observed that when new ball surfaces are run together under load, at a speed producing a relatively low average voltage across the contact, that the voltage reading will increase with running time to a preliminary stabilization level. Data on such runs are presented on Enclosure 15. A preliminary stabilization level usually occurs in a relatively short time period of 60 to 90 minutes. Even after this period, further very gradual increases in contact voltage are noticeable over longer periods of time. This may be seen by comparing Enclosure 6 with Enclosure 7 where Enclosure 7 is a re-run with the same balls as Enclosure 6. It is seen that for any given load, a given voltage is reached at a lower speed with the re-run balls. Approximately six hours running time occurred between the start of one test and the start of the second test. It is not yet known whether secondary stabilization occurs or whether the voltage continually approaches 100 mv. It has been concluded on the basis of the curves shown and also from examinations of the balls after running, that the initial stabilization period is a result of improvements in surface finish by metal removal and/or permanent deformation.

Of some interest is the curve shown for etched balls and the special Esso lubricant. The voltage curve for these etched balls shows dips. It was determined that these were the result of shifting of the top ball track position. Based upon this test it was concluded that the upper ball must be bonded to the spindle (in future testing the ball will be retained with a specially designed nut to facilitate test ball changes). In all of the testing conducted, it was noticed that no tracks appeared on the lower balls. Tests were then conducted on four-ball machines used for endurance testing, and it was determined that approximately 150 lb. load is required in order to show tracking on the lower balls in long running. These tests are not directly comparable to the conductivity tests, in that the speed was held constant, whereas, in the conductivity testing the speed is constantly being varied. It is intended to carefully evaluate lower ball tracking, since significant differences may be observed if both upper and lower ball surface finishes are improved.

Ball Examination After Running. Enclosure 16 shows Talyrond and Talysurf traces over the upper ball track after running through the two complete final test series, and microphotographs of a portion of the same ball track. A depression has been generated which is about 18 thousandths of an inch wide and, at maximum depth, 15 millionths of an inch below the original spherical surface. Both the Talyrond and Talysurf traces indicate the displacement of material to either side of the depression. The Talysurf traces indicate a definite improvement in the surface finish in the deformed area.

Enclosures 17a and 17b show micrographs at 100X and 1000X respectively. Their orientation on the ball is shown in the sketch of Enclosure 17a. Bands of fretting corrosion are visible on either side of the track. It appears as though three distinct bands make up each of the larger bands. It is assumed that the fretting results from the sliding which occurs in the lightly loaded peripheral regions of the contact. The sub-divisions of the bands may result from the fact that the load was applied in increments. The areas within the contact appear to have been improved in surface finish in that the lapping scratches have been greatly reduced in number and depth. Throughout the contact area and into the bands of fretting corrosion themselves, the surfaces contain horseshoe shaped markings in great numbers. These markings are, as yet, unexplained. They are quite regular, in that the open end points generally toward the major ball diameter which is parallel to the track, are smallest in the center and largest toward the outside edges of the track. The markings appear to have been formed mechanically, however, the radii seem much too small to have been formed by one ball pivoting about the other.

2-4 Discussion of Results

In order to understand better the meaning of conductivity test results, it is recalled that conductivity testing, as attempted here, is based on the work by Furey (39). It is Furey's contention that contact, as evidenced by current under the low DC voltages used here, indicates a metallic contact between the rolling surfaces. He states that for lubricants without EP additives the absence of current indicates complete separation by a full lubricant film. His oscillograms have tended to show that at any given time, contact is made or broken in a series of discrete steps of either zero voltage or full voltage across the contact. He concluded from this that there are only two conditions in the contact zone: either full film or metallic contact at least at one point.

The test results reported here have not completely substantiated this concept in that the oscilloscope traces appear to show dwell periods of the voltage at intermediate levels. It can be argued that these dwells are artifacts due to the response characteristics of the electronic system, but this cannot be proven at this time. At the present time, therefore, there is a possibility that intermediate stages exist between full contact (metallic contact) and full separation, caused either by dielectric breakdown of an oil film having less than a given minimum thickness capable of withstanding the voltage applied, or in turn caused by contact between the surfaces with an interposed boundary layer, oxide film or other high resistance material which causes a high contact resistance to exist.

Whatever the mechanism of these intermediate conditions might be, it seems safe to assume that full voltage across the contact (100 millivolts in our case) indicates a full film. For this reason, the points on the average voltage vs. speed curves where the curve reaches 100 millivolts can be taken to be indicative of the establishment of a full, uninterrupted lubricant film.

On the other hand, the low speed region at which no detectable voltage is observed can be taken to signify the absence of a full lubricant film. It does not necessarily follow that at these low speeds there is true metallic contact, part or all of the time, but it seems clear that a different situation exists from that characterized by a 100 millivolt voltage across the contact.

In the intermediate speed zone where the average voltage across the contact is a finite value other than 100 millivolts, it is very likely that most of the time the Furey mechanism of alternating establishment and disruption of a full film does prevail. This is suggested by the fact that the voltage crosses over the 50 millivolt line regularly and in a countable manner with frequencies shown in the count rate curves. These frequencies seem to be characteristic of the particular test conditions. However, there is a good possibility that there are transition periods between full film and full contact which are characterized by breakdown of very thin films, by the interposition of high resistance layers, or by a multitude of other possible mechanisms. While it appears, therefore, to be safe to assume the existence of a full film of

elastohydrodynamic character for the high speed zone characterized by 100 millivolt voltage across the contact, and of no hydrodynamic film for zero voltage, no definite statement for the intermediate speeds can be made.

One obvious test that suggests itself for further clarification of the occurrences in the contact is to run with a lower applied voltage across the contact. If curves of percent average voltage and count rate then obtained, follow the ones obtained at the higher applied voltage, then it would seem reasonable to assume that dielectric breakdown phenomena of finite thickness films are of minor significance. This test will be conducted in the next period. There is some reason to assume that the test, when conducted, will yield positive results because Furey in his work has performed such tests, and he has found that the applied voltage did not influence the results, providing only that it was low enough. By analogy with Furey's tests, it has been concluded that 100 millivolts should be low enough voltage for the configuration used in the present test. However, this will be ascertained by reducing the voltage further and noting the results.

It should be borne in mind that for film thicknesses predicted by elastohydrodynamic theory and experimentally found by other workers (Sibley et al (16), Archard et al (38)) which are of the order of 5 to 10 microinches, the electric field intensity for 100 millivolts applied voltage, is in the order of 10 to 20 kv/in. At asperities the film thickness is less, and the field intensity will be considerably higher. The dielectric strength of oils tested here is not known. However, the dielectric strength of straight hydrocarbon transformer oils in bulk is of the order of 275 kv/in. If bulk dielectric strength is a guide to the strength in thin films, even thin points on the film, say of the order of 2-3 microinches, would be successfully isolated under 100 millivolts applied voltage.

The count rate curves shown are of interest as indicating the frequency of film breakdown occurrences. As can be seen in the enclosures, count rates up to 250 per rolling cycle have been observed. It follows from the geometry of the test arrangement that about 1.34 revolutions take place before a given lower ball twice rolls over a point on the upper ball. There are, accordingly, up to

250 film interruptions while the monitored contact travels once around the upper ball. Under these speed and load conditions, therefore, the film is highly unstable. At maximum count rates, several contacts are made or broken while the contact travels a distance equal to one Hertzian diameter.

The conductivity testing will make it possible to select test conditions for endurance tests in the rolling 4-ball configuration, in which there exists a continuous hydrodynamic lubricant film, and others in which there is none (continuous contact). As soon as such conditions have been verified with conductivity testing at practical endurance testing speeds and loads, it is planned to initiate endurance runs under a pair of such conditions, in order to gather data regarding film influence on fatigue life.

3

AUTORADIOGRAPHY OF FOUR BALL TEST SPECIMENS

3-1 Autoradiography Techniques

The autoradiography of ball specimens from rolling 4-ball tests using one activated lower ball presents a considerable experimental problem. The autoradiographic film has to conform closely to the spherical ball surface, especially in the region of the wear track. Gaps of 2 to 3 microns have been shown to impair resolution materially (40). The wear tracks themselves are rather narrow (about 300 microns for 500,000 psi contact pressure). To detect the location of transferred wear particles across a wear track of this width, autoradiography with a resolution of well below 100μ has to be employed. The fast X-ray films generally employed in wear studies have, under the most favorable conditions, a resolution of about 50μ (with pure beta emitters of high specific activity, and under ideal geometric conditions such as perfectly flat surfaces).

The best approach to high resolution autoradiography on test balls under conditions of difficult geometry and in the presence of gamma emitters appears to lie with very thin films such as the 10μ thick Kodak Autoradiographic Stripping Film, Type NTB and the 5μ thick Kodak Autoradiographic Permeable Base Stripping Film. These films are applied to the specimen by flotation techniques which assure very close and uniform contact between the specimen and the radiation sensitive emulsion. Unfortunately the application of the film to the specimen has to be carried out in water with the resulting danger of corrosion on the steel ball specimen. Rust will give rise to autoradiographic artifacts, such as abrasion of the emulsion by rust particles during the oxidation of iron to iron oxide.

Prior to the start of radiotracer experiments a technique was checked out to coat steel balls with a water impermeable film (41). To prevent large scale absorption of beta radiation by an interposing protective layer between specimen and emulsion this protective layer has to be extremely thin, preferably one micron or less.

By applying one drop (0.05 ml) of a 1% by weight Saran F-120 solution in methylethyl ketone concentrically to the topmost point on a 1/2 inch ball (that is the drop is applied at the "north pole") the upper hemisphere can be covered with a continuous water-impermeable

film. Coated balls were tested for protection by dipping into dilute nitric acid. Uncoated areas of the balls are etched immediately, while the coated areas were not affected at all by a 10-20 second dip in nitric acid. The completeness of film formation on a steel ball can be followed readily by the appearance of interference colors ranging from yellow to blue depending on the thickness of the film. Assuming that all of the solution applied stayed on the upper hemisphere, the obtainable film thickness from one drop of the solution used can be calculated to be about one micron. Allowing for some run-off of solution (which actually does occur) the films prepared on 1/2 inch balls are below one micron in thickness and are continuous enough to protect the balls against temporary exposure to water and moisture.

As a next step, the Kodak Autoradiograph Permeable Base Stripping film was floated on to a ball pre-coated with Saran film. Careful examination under a Stereo Microscope indicates that the floated emulsion covers sufficiently large zones of the ball with a wrinkle-free, tightly adhering film. Thus, the mechanics of film application appear to be solved.

It is intended to coat a small spherical electric light bulb with an opaque layer, and produce fine pinpoints or scratches on this layer. Next, a Saran film and a Kodak strip film will be applied and the latter exposed by lighting the bulb. It is expected that the results will yield an evaluation of the resolution obtainable by this process.

Another approach to high resolution autoradiography being investigated for metal transfer studies is the use of lightly carburized surfaces, using a C-14 containing gas as the carburizing atmosphere. The introduction of C-14 into bearing surfaces is believed to improve autoradiographic resolution two fold by (1) limiting radioactivity to a pure beta emitter, thus eliminating interference from scattered gamma radiation, and (2) permitting the use of bearing surfaces with higher specific surface beta activities than is practicable with neutron activated steel specimens. This approach has not yet been followed up.

3-2 Test Preparations

The initial phase of radiotracer testing will be conducted with a specially adapted four ball test machine. The modifications consist primarily of special handling facilities and shielding to eliminate radiation hazards.

Testing for the next period will be in two parts. The preliminary testing will consist of tests to determine the amount of transfer which may be expected under conditions of intimate metallic contact. Tests will then be conducted to determine the transfer which will occur during acceleration of the test rig to the speed giving a full lubricating film. Attempts will be made to minimize transfer during this time by accelerating under low load. The full film test point will be established from conductivity tests. After accounting for the acceleration period, tests under full film conditions will be run. If it is shown that no transfer of material occurs under these conditions, the test speed will be reduced until metal transfer takes place. Thus, the radioactive testing will verify the existence of a full film, and will also provide a means of calibrating the full film point, by yet another means. (It is possible that the full film point is established sooner than indicated by the voltage measurements.)

If it is found that too much metal transfer occurs during the acceleration period, a specially designed cup will be fabricated which will make it possible to change the contact angle of the four ball configuration while in operation by changing the pitch diameter of the cup. In this manner, the rig may be brought up to speed under load under one contact angle, and then shifted to a new contact angle so that a fresh contact area is exposed.

Two other test machines are being modified for radioactive testing. These are an R2 test machine for ball and roller bearing testing, and a flat washer machine for testing balls against flats.

4

LUBRICANTS FOR THE HYDRODYNAMIC STUDIES

4-1 Types of Lubricants

Some of the lubricants to be used in the present studies are selected high temperature lubricant formulations. These materials furnished to [redacted] Industries are of known composition and have been found previously to possess certain qualities desirable of high temperature lubricants.

The materials to be used comprise the following general classes of compounds:

Diester Formulation (MLO-7593) (from Penn State University)

Polyolefin (MLO-7584) (from Penn State University)

Highly refined Naphthenic Oil Formulations: MLO-7582, 7277, and 7451 (from Penn State University), the base oil for the preceeding three formulations (from Esso Res. and Eng), MLO-7558 (from Esso Res. Eng.)

Paraffinic Resin Extract (MLO-7583) (from Penn State University)

Polyphenyl ether (MLO-7503) (from Monsanto Chemical Co.)

Silicone Lubricant (MLO-7017) (from General Electric Co.)

Enclosure 18 lists the exact compositions of the formulations outlined above. Their general properties are discussed below.

The diester formulation (MLO-7593) is basically a turbo-jet engine oil of the type used in applications requiring conformance with specification MIL-L-7808. Due to the special additive package incorporated this formulation has better high temperature properties than the usual MIL-L-7808 oils. In fact, it fulfills all bench test requirements of the high temperature turbo-jet engine oil specification MIL-L-23699.

The polyolefin (MLO-7584) is a special cut of polyisobutene manufactured by the Standard Oil Company of Indiana. Its physical properties are comparable to the commercial product Indopol-L50.

MLO-7584 has a considerable capacity for oxygen uptake due to the large number of carbon-carbon double bonds in the molecule. The oxidation products of MLO-7584 are high volatility materials. Hence this lubricant does neither thicken nor coke (as readily as more conventional lubricants) at high-temperatures.

Three of the formulations based on a highly refined naphthenic oil (MLO-7582, 7277 and 7451) are designed to study the effect of E.P. additives on rolling contact lubrication at high temperatures. MLO-7582 is an oxidation inhibited base oil, MLO-7277 is tricresylphosphate containing MLO-7582 formulation and MLO-7451 consists of a MLO-7582 base stock containing an E.P. additive of the acid phosphite type.

The tricresylphosphate containing formulation has been submitted to Wright Air Development Division by the Petroleum Refining Laboratory of Pennsylvania State University as a high temperature hydraulic fluid under the designation MLO-7243 (42).

Primol 355 and MLO-7558 are straight naphthenic base oils containing only a trace amount of preservative to increase the storage stability of the materials (Primol 355 is the base stock for MLO-7582, 7277 and 7451). The above two additive-free base oils are used for preliminary conductivity studies in order to eliminate all possible interference by additive packages with the conductivity techniques used in this work. Furey (39) has shown that certain EP additivies create non-conductive bonded films which, in conductivity work, simulate hydrodynamic separation. Bulk data for these base oils proper are not available; the data given were obtained from Esso Research and Engineering and refer to blended formulations containing various additives of an unspecified nature.

The paraffinic resin extract (MLO-7583) is a high viscosity material with certain desirable high temperature properties. Though its thermal stability at 600 and 700°F is inferior to lower viscosity paraffinic oils, the heavier material shows less tendency towards dirt (coke) formation under high temperature oxidation conditions (43). This material has a viscosity of about 9 centistokes at 400°F as compared to viscosities of 2 cs or less for most other oils in the test program.

The polyphenyl ether, MLO-7503, is a member of a new class of high temperature lubricants. The polyphenylethers have been shown to have good lubricity characteristics and oxidation stability at temperatures where conventional lubricants become unusable. The polyphenyl ethers are also quite resistant to radiation damage (44).

The silicone lubricant to be used in the present studies (MLO-7017) is a chlorinated material, General Electric Versilube F-50. This material has somewhat improved lubricity properties as compared to methylsilicone lubricants.

In addition to the above oils, a medicinal grade white oil (Nujol) has been used in the conductivity studies. Since this material is not used as a lubricant in the conventional sense, standard engineering data are not available. Nujol is a straight hydrocarbon oil without any additives.

4-2 Lubricant Properties

The available specific information on the properties of the lubricants to be used in the present program is tabulated in Enclosures 19-28.

The viscosity-temperature properties are listed in Enclosure 19 and are self-explanatory.

The viscosity-pressure relationships from 200-1000 psig* are tabulated in Enclosure 20. The data listed were obtained by the Petroleum Refining Laboratory at Pennsylvania State University (42) with a modified shear viscometer. Pressure coefficients in this pressure range are unobtainable by the "Falling Ball" method. Preliminary data indicate that the two methods do not correlate below 10,000 psig (45).

Interesting to note in Enclosure 20 are the viscosity measurements on gas saturated oils at 1000 psig and 100°F. In several instances the viscosities of the gas saturated oils dropped below the values for the same oils at atmospheric pressure. The effects of gas solution on viscosity at high temperature and high pressures is presently unknown.

---

*Viscosity-pressure data at higher pressures are unavailable.

Bulk modulus (coefficient of compressibility) data for the lubricants under discussion are presently unavailable.

Density-Temperature data and Coefficients of Expansion are listed in Enclosures 21 and 22 respectively.

Thermal Conductivity and Specific Heat data are found in Enclosure 23.

Vapor Pressure-Temperature relationships, where available, and Evaporation Test data are listed in Enclosure 24.

Some Electrical Properties were obtainable for the polyphenyl ether and are listed in Enclosure 25.

Thermal Stability Test data are assembled in Enclosure 26. Outstanding in its thermal stability at 700°F is the polyphenyl ether fluid (MLO-7503). The highly refined mineral oil formulations (MLO-7582 and 7277), while inferior to polyphenyl ethers and silicones in thermal stability, show a marked improvement over the ester based oil (MLO-7593). The latter solidifies completely after 6 hours at 650°F, the mineral oils remain fluid after that time at 700°F.

Oxidation-Corrosion Stability Test data, Enclosure 27, show a similar trend. The outstanding fluid in this test at 500°F is again the polyphenyl ether.

Unfortunately, available data on the oxidation characteristics of the lubricants for this program, have been obtained under a variety of conditions, such as time and temperature, making detailed direct comparisons somewhat difficult.

Lubricity data from Shell 4-Ball Wear Tests are shown in Enclosure 28. Of significance to the lubrication studies are the results from the four mineral oil formulations. The naphthenic mineral oil (MLO-7582, 79 cs at 100°F) ranks lowest in the group in the 4-Ball Wear Tester at 67°F (75°C), 620 rpm and loads from 1 kg to 40 kg. The paraffinic resin (MLO-7583, 3836 cs at 100°F) and the mineral oil plus 0.5% di-isopropyl acid phosphite formulation (MLO-7451) are about equivalent, the latter being somewhat superior at 40 kg load. Mineral oil plus 1.0% tricresylphosphate ranks highest of the mineral oil formulations.

The ester fluid (MLO-7593) as well as the silicone formulation (MLO-7017), while showing fairly low wear at 1 kg and 10 kg loads and moderate temperatures, rapidly deteriorate in their lubricating ability at 500 and 600°F and 40 kg load.

5

HYDRODYNAMIC FILM MEASUREMENTS UTILIZING X-RAY TECHNIQUES

It has been outlined in the first progress report, that X-ray beam techniques will be used to obtain film thickness and film shape data by absolute measurements.

In order to better understand and predict the performance of the X-ray measurement method, utilizing two balls in contact, considerable emphasis has been placed on continued experimental and analytical studies of X-ray beam optics. This testing has confirmed the feasibility of using a direct beam measurement method. It is anticipated that testing during the next reporting period will finalize the evaluation of the direct beam technique. Evaluation of the performance of the curved crystal technique described in Progress Report No. 1 will commence. The X-ray beam studies are discussed in detail later in this section.

5-1 Mechanical Design of the Two Ball Test Machine

The basic design of the two ball test machine was described in Section 2-1 of Progress Report No. 1. The majority of the design details have been completed and preparations are being made for obtaining bids prior to fabrication.

The major area of design which has not been finalized is the X-ray beam system. A preliminary design for the curved crystal system has been prepared and will be fabricated and pre-tested in the static device. An arrangement for the direct beam method will be designed in the next period.

The initial motor drives are being sized for operation of the spindles at 5,000 rpm. This speed has been chosen on the basis of cost and the availability of equipment. If it is found necessary to operate at higher speeds it will be necessary to switch to more elaborate drives and controls than are now being contemplated. The design has been arranged so that no re-design of the test machine itself will be required other than the addition of larger motor mounts.

5-2 X-ray Measurement of Oil Film Thickness

The primary problem in achieving accurate film thickness measurements by X-ray transmission between two balls lies in the accurate calibration of measured X-ray intensities to permit the computation of corresponding values for the oil filled separation between the balls.

In order to obtain valid results from an X-ray system the following requirements must be met:

1. Calibration of X-ray intensity vs. separation must be independent of the geometry of the contact area.

2. The technique must be sensitive to separation differences in the order of 1 microinch.

3. Background level (counts per second measured at zero separation) must be low. A certain amount of background is unavoidable, its causes and methods for elimination will be discussed later.

Calibration. A detailed presentation of the method of calibrating intensity as a function of separation appeared in the Progress Report No. 1, however, a brief review is now given:

The X-ray beam is directed at the interface between two accurately finished 1" diameter balls in dry contact under no load. The contact point is then determined by finding the point of minimum X-ray intensity. This minimum intensity value is called "background" and is subsequently subtracted from all the readings. With the contact point known it is possible to calculate from geometry the separation at any measured distance from the contact point, see Enclosure 9, Progress Report No. 1. Intensity can now be plotted as a function of separation and a calibration is obtained for separations ranging from 0 microinches to as high a value as desired. In practice, calibration trials are run between 0 and 500 microinches.

X-ray Beam Geometry. Design work is in progress on the X-ray system described in Progress Report No. 1 utilizing two lithium fluoride single crystals but it has not been investigated experimentally to date. The techniques for grinding and bending single crystals have been discussed in private communications (46), and a LiF single

crystal slab, 1" x 3", has been ground successfully to 1 mm thickness in preparation for bending to the proper radius. This system, upon completion of the necessary parts, will be tested and calibrated and results compared with the two experimental X-ray beam arrangements that have been investigated before. Both of these arrangements, described below, involved use of an undiffracted beam of strong characteristic Molybdenum K radiation with accompanying white radiation.

a) The first arrangement investigated made use of the direct beam with the line-shaped focal spot of the X-ray tube lined up parallel to the line between the centers of both balls. Divergence in the direction of the two ball centerline was limited by means of parallel plates placed as shown in Enclosure 29A . Results using this method are given in Progress Report No. 1, Enclosures 6, 10, 11, 12 and 13, where the nonlinear intensity vs. separation calibration can be clearly seen.

b) A much more effective use of the direct beam is accomplished by the second method investigated, originally proposed by a consultant (46). Here, Enclosure 29B, the line focus of the X-ray tube is oriented horizontally and is viewed at right angles to its length. In discussing Enclosure 29 vertical is understood to mean in a direction parallel to the centerline between the balls while the horizontal plane is perpendicular to this centerline. Both vertical and horizontal divergences are initially limited by a long aperture which effectively encloses the entire beam in a tube. An adjustable vertical slit formed by two short parallel plates placed close to the balls limits the horizontal divergence so that the rays can be considered as contained in a vertical plane passing between the jaws of the slit. In this way the radiation, once past the vertical slit, can be considered as a "sheet" of rays emanating from a "point" source. The length (horizontal dimension) of the "point" source is limited to the length of the line focus that can pass rays through the vertical slit. The height of the "point" source (its dimension parallel to the direction in which separations are measured) depends on the breadth (.8 mm) of the focal line and the angle (6°) at which this breadth is observed (the take off angle). Enclosure 30 presents diagramatically the geometry by which intensity increases with separation assuming that radiation comes from a point source. The divergence angle δ defines

the amount of radiation passing between the balls and keeping in mind the fact that separations are on the order of microinches compared to a source to ball distance of several inches it is apparent that δ is extremely small. Since the sine of a small angle can be approximated by the angle (in radians), δ increases linearly with separation and therefore the relationship between intensity and separation is linear.

It is evident from the discussion above that considering the X-ray source as a mathematical point is a rough approximation since in fact the "point" source is quite large with respect to separations on the order of microinches. A special report is being prepared at this time to include an analysis of the geometrical optics involved. An analysis of the relationship of intensity with separation for various assumed contact area sizes will be included. The errors introduced by applying calibration data from undeformed balls to contact area situations is also being investigated. Results already available indicate that linearity for the geometries expected is good and that effects of contact area dimension are minor.

5-3 Experimental Data

It must be shown experimentally, that the background and intensity requirements can be met. Two ball contact profiles were determined and the effect of the following variables on both background and intensity were examined:

1. Type of radiation counter
2. Selective filters
3. Slit width

Type of Radiation Counter. The counting efficiencies (ratio of photons counted to photons received) of radiation counters generally vary with the wavelength of impinging radiation. It is important, therefore, to use a counter that has a high counting efficiency for the X-ray wavelength being used. Data published by G.E. (47), show that, for MoKα (0.711Å) radiation, either a krypton or a xenon filled proportional counter is a good choice.

The krypton filled proportional counter was initially chosen since the efficiency vs. wavelength data show that it is more selective

in its acceptance of wavelengths, i.e. it has a high counting efficiency for MoKα radiation with a rapidly decreasing efficiency for shorter and longer wavelengths. This effect was considered valuable since the counter would selectively ignore radiation coming from the two following possible background sources.

1. Short wavelengths which penetrate the material of the balls.

2. Long wavelengths coming from iron fluorescence.

These background sources will be examined in more detail later, at this time it is sufficient to say that serious background problems were encountered with the krypton filled counter as shown in the following data.

Enclosure 31 is a plot of the X-ray intensity, that passes between the balls, as a function of distance from the contact point (the point of minimum intensity). The curve was obtained by step-wise scanning across the profile of the two ball contact area in a direction perpendicular to the line between the centers of both balls and the abscissa values are given as distance, measured in this direction, from an arbitrary reference point. Intensity was measured with the krypton proportional counter under the following conditions:

Pulse Height Selector: All pulses above 5 V accepted (this setting does not represent an attempt at monochromatizing the beam, it merely eliminates random noise pulses produced by the circuitry)

Filters: no filters were used

Slit Width*: .0008" $\pm$ .0002"
(*refers to the slit directly in front of the balls)

Power Supply to the X-ray tube: 45 KV 22 MA

The point of minimum intensity corresponds to the contact point where separation is zero. A plot of X-ray intensity against separation (separation is calculated as previously described under "Calibration") is given in Enclosure 32 . By extrapolation, zero intensity is found to occur at a "negative separation" of 195 microinches. The "negative separation" thus found will now be defined as background level, and the counting rate which occurs at a known zero

separation can be expressed as microinches of apparent separation. Obviously since oil film thicknesses on the order of 10 microinches are anticipated in dynamic film measurements this background level is totally unacceptable. Enclosure 33 , a plot of counting rate above background per microinch separation as a function of separation, shows, however, that the counting rate increases nearly linearly with separation, thus the geometrical picture given in Enclosure 30 is correct as a first approximation.

A drastic reduction of background intensity was obtained by changing from a krypton filled to a xenon filled proportional counter. Enclosure 34 shows the two ball contact profile measured with the xenon filled counter under the following conditions:

Pulse Height Selector: All pulses above 5 V accepted

Filters: none

Slit Width: .0008" ± .0002"

Power Supply to the X-ray tube: 39 KV 24 MA

The intensity vs. separation curve of Enclosure 35 shows that background level has been reduced to 21 microinches, and Enclosure 36 indicates a linear increase of intensity with separation over the entire range from 0 to 500 microinches. A comparison between Enclosures 33 and 36 shows that this improvement in background level was achieved with no appreciable change in the intensity (count rate per microinch separation).

No satisfactory explanation can be given for the drastic difference in background levels found for these two proportional counters. It has been observed however that krypton gas is excited by wavelengths below 0.865 Å (which includes MoKα radiation) causing the gas itself to become a source of radiation (fluorescence). This phenomenon does not occur in xenon at wavelengths above 0.385 Å and since the wavelengths present in the incident beam are predominantly above this value, fluorescence of the xenon gas is practically eliminated. This point is mentioned since it had been suggested by counter manufacturers that it may have some bearing on the background and was, in fact, the basis for changing from a krypton filled to xenon filled counter.

Pulse Height Analysis of Background Radiation. At this point an effort was made to determine the source of the remaining background radiation. The following are some sources of background which were suspected.

1. Iron Fluorescence When an element is irradiated by X-rays with an energy level above its excitation edge it becomes a source of X-rays itself or is said to fluoresce. In the case of steel balls, iron K radiation is excited in the balls by the impinging molybdenum K radiation. This fluorescent radiation travels in all directions and could enter the counter.

2. Radiation Penetration through the Balls A certain amount of radiation penetrates the material of the balls and reaches the counter giving an apparent separation greater than that which exists. If monochromatic MoKα radiation is considered, the apparent gap contributed by this transmitted radiation has been calculated for perfect spheres in unloaded contact, see Enclosure 37 , to be approximately 2 microinches. The apparent gap which would be produced by monochromatic X-rays at the short wavelength cut off value (for X-ray tube operating at 45 KV) is on the order of 200 microinches. Thus hard X-rays in the white radiation spectrum, although a small proportion of the total radiation energy generated by the tube, contributes a disproportionately high background level.

3. Horizontal Divergence Some beam widening, which depends on the amount of horizontal divergence, occurs after the beam passes through the slit in front of the balls. Since unloaded balls (except for top ball weight) make contact over a very small area, obviously some radiation will reach the counter if the beam has any appreciable width.

These three factors were considered the prime suspects as sources of background intensity and the wavelength relationship between them is as follows:

1. Iron fluorescence occurs predominately at 1.94 Å

2. Radiation penetrating through the balls is concentrated at the shortest wavelengths below MoKα wavelength

3. Background caused by horizontal divergence occurs at the same wavelength as the incident beam; primarily MoKα radiation

(0.71) Å).

In order to determine the relative importance of these factors in causing background a wavelength analysis of the background radiation was done by making use of the relationship between the pulse height generated in the counter by an incoming photon and its wavelength (48). This relationship is characterized by a distribution of pulse heights about some mean value for a given X-ray wavelength. The pulse height mean value is proportional to the energy of incoming photons and it is possible to distinguish between wavelengths entering the counter by means of a single channel pulse height analyzer. Some inferences as to the source of background may be made by comparison of the background radiation pulse height distribution with that of the direct beam.

Examination of both pulse height distributions, Enclosure 38 , indicated that the wavelength distribution of background radiation was nearly identical to that of the direct beam with a slightly higher proportion of short wavelength radiation being present in the background.

This indicated that the primary background problem was caused by horizontally divergent rays with a minor contribution to background coming from the highly penetrating short wavelengths. There was no indication of any appreciable concentration of pulses in the area corresponding to the characteristic iron fluorescence wavelengths. In order to verify the conclusions drawn from this comparison, calibration trials described in the following sections were conducted.

The Effect of Filters. The conclusion drawn above, that iron fluorescence gives an insignificant contribution to the background intensity, was substantiated by placing aluminum filters over the counter tube window. Iron fluorescence is highly absorbed by aluminum while Mo characteristic radiation travel through it rather readily, thus a 2.3 mil aluminum filter stops over 75% of the iron fluorescence while allowing 93% of the Mo radiation through. If iron fluorescence made any significant contribution to the background problem we could expect filtering to produce a sharp drop in background intensity with only a slight loss of signal intensity. No significant change in background level was observed, however, and iron fluorescence was eliminated as a possible source of background problems.

Slit Width. Horizontal divergence, which was shown by pulse height analysis to be the prime cause of background, can be controlled by the slit in front of the balls. The slit actually consists of two parallel flats and Figure 1 of Enclosure 39 shows schematically how the beam width, B, is defined at the plane P, shown in Enclosure 29 B , which is the vertical plane that cuts through the center of the balls and is perpendicular to the X-ray beam. The derivation given below Figure 1 shows that for a fixed slit width, W, and a given distance, A. between the slit and the plane P, beam width varies directly with slit opening.* Figure 2 of Enclosure 39 is a drawing of the beam with width, B, striking the balls at plane P. Separations are at a minimum in this plane and the blacked in area of Figure 2 represents the cross section of the beam that passes between the balls at 0 separation as a result of beam width. The derivation given below Figure 2 shows that this area varies with the cube of the beam width which in turn varies directly with slit opening. Since the intensity observed passing between the balls is a function of this area, a very small decrease in slit opening has a powerful effect on background at 0 separation and this conclusion is supported by the following data.

Enclosure 40 shows the profile obtained under the same conditions as Enclosure 34 with the exception that slit width was changed from .0008" to .0005". A background level of 5 microinches was realized with the smaller slit width as shown in Enclosure 41 . The small slit opening gives a count rate of approximately 1.9 counts per second per microinch compared to a value of 7.7 counts per second per microinch obtained at the wider slit opening. This loss of intensity requires the use of long counting times, however, both the background level and counting rate obtained are feasible for successful film thickness measurements. Reasons for the sharp drop of the count rate for reduced slit width will be apparent from the mathematical analysis of the X-ray geometry, to be given in a special report.

5-4 Summary of Results and Future Plans

The assumption is implied in the above discussion, that background can be determined by simply measuring the radiation level at zero separation and subsequently subtract it from all other readings. This is by no means completely satisfactory.

The problem of mathematical compensation for background is illustrated by the following:

*Total reflection is neglected in this discussion.

a) Radiation penetrating through the balls - This portion of the background radiation depends on the path length of steel through which radiation must traverse as well as the wavelengths present in the incident beam. In the case of undistorted balls under no load, the path length is constant and the error can be calculated. Under load, however, path length will increase and the background is considerably diminished. Fortunately the contribution to this source of background by short wavelengths can be removed by pulse height discrimination which eliminates pulses generated by short wavelengths. The remaining background level caused by penetration through the balls has been shown to have a maximum value of 2 microinches, Enclosure 37 , therefore, the error in uncorrected oil film measurements is not too great.

b) Intensity due to total reflection - At low glancing angles X-rays will reflect totally from a surface in a manner analogous to the total reflection of visible light from a surface within a prism. This portion of the observed intensity varies with the geometry of the contact area, and will be dealt with in the forthcoming special report.

c) Beam width errors - The intensity of radiation measured depends on the cross sectional area of the beam which passes between the balls but is interpreted as the average height of that area. For a sufficiently narrow beam the average height will not differ appreciably from the height at the center of the beam. In a calibration trial this difference only becomes important when the beam is near the point of zero separation in which case the average height of the cross section gives an apparent separation that does not exist.

It is apparent that a straight subtraction of the background count is arbitrary. The safest method for applying calibration results to film measurements certainly lies in reducing background to a minimum where corrections are unimportant.

The most effective background reduction was achieved by changing from a krypton to a xenon filled proportional counter and by limiting horizontal divergence by means of the vertical slit in front of the balls. Iron fluorescence was shown to make a negligible contribution to background. Minor reductions in background were

achieved in the course of experimentation by reducing the voltage applied to the X-ray tube and limiting the acceptance of high voltage pulses. Both of these are methods for eliminating the background contribution from highly penetrating X-rays in the high energy portion of the white radiation spectrum. Since the background contribution from this source was small when compared to the effects of beam widening its effect was largely masked in previous experimentations and the optimum conbination of X-ray tube voltage and pulse height acceptance remains to be determined.

In view of the demonstrated importance of restricting horizontal divergence a new slit has been designed. It consists of two parallel flats approximately 1 inch long ,(W of Enclosure 39) and will be built up from gauge blocks, providing slit widths that can be varied in increments of 0.0001". This redesigned slit used in conjunction with a xenon proportional counter, optimum X-ray tube power settings, and pulse height acceptance should produce the best data available with direct radiation methods.

Also considered will be the possibility of using a calibrating configuration other than unloaded balls in contact. This configuration, due to the small contacts obtained is, in fact, rather unlike a loaded contact. An attempt will be made to calibrate through an opening between flat surfaces, giving long gaps similar to those expected in loaded ball contact with hydrodynamic films.

REFERENCES

1. Barwell, F. T., "Effect of Lubricant on Pitting Failure of Ball Bearings", Engineering, July 6, 1956, pp. 9-12.

2. Sibley, L. B., and Austin, A. E., "An X-Ray Method for Measuring Thin Lubricant Films Between Rollers", Instrument Society of America, Preprint No. 65-LA-61 (1961).

3. Reynolds, O., Trans. Roy. Soc. 177 (Pt. I). (1886).

4. Martin, H. M., "The Lubrication of Gear Teeth", Engineering 102, 119, 1916.

5. Hertz, H., "Miscellaneous Papers", Macmillan, London (1896).

6. Lundberg, G., and Palmgren, A., "Dynamic Capacity of Rolling Bearings", Acta Polytechnica Mechanical Engineering Series, 1 (3), 7 (1947), and 2 (4), 96 (1952).

7. Cordiano, H. V., Cochran, E. P., Wolfe, R. J., "Effect of Combustion Resistant Hydraulic Fluids on Ball Bearing Fatigue Life", ASME paper no. 55-LUB-21 (1955).

8. Morrison, T. W., "Some Unusual Conditions Encountered in the Lubrication of Rolling Contact Bearings", Lubrication Engineering 11 (6), (1955).

9. Wolfe, R. J., and Berkson, W. G., "Influence of Aircraft Gas Turbine Lubricants on the Fatigue Life of Heavily Loaded Angular Contact Ball Bearings", Project 5912-1, Final Report NS 074-001.

10. Otterbein, M. E., "Effect of Aircraft Gas Turbine Oils on Roller Bearing Fatigue Life", ASLE, 1957, Preprint No. 57 LC-9.

11. Jackson, E. R., "Rolling Contact Fatigue Evaluation of Bearing Materials and Lubricants", ASLE/ASME, 1958, Preprint No. 58 LC-15.

12. Anderson, W. J., and Carter, T. L., "Effect of Lubricant Viscosity and Type on Ball Fatigue Life", ASME (1958).

13. Baughman, R. A., "Experimental Laboratory Studies of Bearing Fatigue", ASME, 58-A-235.

14. Crook, A. W., "The Lubrication of Rollers", Phil. Trans. Roy. Soc., London, 250, 387-409, 1958.

15. MacConochie, I. O., and Cameron, A., "The Measurement of Oil-Film Thickness in Gear Teeth", Journal of Basic Engineering, ASME, 82 (1), 29 (1960).

16. Sibley, L. B., and Orcutt, F. K., "Elastohydrodynamic Lubrication of Rolling-Contact Surfaces", ASLE Transactions, 4 (2), 234-249 (1961).

17. Dowson, D., Higginson, G. R., "A Numerical Solution to the Elastohydrodynamic Problem", J. Mech. Engr. Science, 1 (1), 6-15 (1959).

18. Grubin, A. N., Vinogradova, I. E., "Investigation of the Contact of Machine Components", Moscow, TsNIITMASh, Book No. 30 (1949), (S. S. I. R., London, Translation No. 337).

19. Cameron, A., "Hydrodynamic Theory in Gear Lubrication", J. Inst. Petroleum, 38, 614 (1952).

20. Dowson D., and Higginson, G. R., "New Roller Bearing Lubrication Formula", Engineering, 192 (4972), 158-159 (1961).

21. Dowson, D., and Higginson, G. R., "The Effect of Material Properties on the Lubrication of Elastic Rollers", J. Mech. Engrg. Science, 2 (3), 188-194 (1960).

22. Archard, G. D., Gair. F. C. and Hirst. W., "The Elastohydrodynamic Lubrication of Rollers", Proc. Roy. Soc., A, 262, 51-71 (1961).

23. Dörr, J., "Schmiermitteldruck und Randverformung des Rollenlagers", Ing-Arch., 22 (3), 171-193 (1954).

24. Dörr, J., University of Saarlands, Saarbrücken, Germany, private communication.

25. Bell, J. C., "Lubrication of Rolling Surfaces by a Ree-Eyring Fluid", ASLE Paper No. 61-LC-17 (1961).

26. Crouch, R. F., and Cameron, A., "Graphical Integration of the Maxwell Fluid Equation and its Application", Inst. Petroleum, 46 (436), 119-125 (1960).

27. Milne, A. A., "A Theory of Rheodynamic Lubrication for a Maxwell Liquid", Proc. of the Conf. on Lubrication and Wear, London, 1957, Published by Inst. of Mech. Engrs.

28. Burton, R. A., "An Analytical Investigation of Visco-Elastic Effects in the Lubrication of Rolling Contacts", ASLE/ASME 1959, Preprint No. 59 LC-1.

29. Kotova, L. I., "Theory of the Rolling of a Cylinder on a Surface Covered with a Layer of the Viscous-Plastic Lubricant", Zh. Tekh. Fiz. 27, 1540, (1957) Trans. in Sov. Phys. Tech. Phys. 2, 1424.

30. Osterle, J. F., "Fluid Lubrication of Roller Bearings", Wear 2, (3), 195, Feb. 1959.

31. Sasaki, T., Mori, H., Okino, N., "Fluid Lubrication Theory of Roller Bearing", Parts I and II, presented at ASLE-ASME Lub. Conf. Chicago, October 19, 1961.

32. Archard, J. F., "The Temperature of Rubbing Surfaces", WEAR, 2, 438-455 (1958-59).

33. Blok, H., Inst. Mech. Eng., 2, 222 (1937).

34. Jaeger, J. C., "Moving Sources of Heat and the Temperature at Sliding Contacts", Proc. Roy. Soc. (New South Wales) 76, 203-224 (1942).

35. Sternlicht, B., Lewis, P., Flynn, P., "Theory of Lubrication and Failure of Rolling Contacts", Trans. ASME, Jr. Basic. Engrg. 213-226, (1961).

36. Howlett, J., "Film-Lubrication Between Spherical Surfaces: with an Application to the Theory of the Four-Ball Lubricant Testing Instrument", J. Applied Physics, 17 (3) 137-149 (1946).

37. Kapitsa, P. L., "Hydrodynamic Theory of Lubrication During Rolling", Technical Physics, 25 (4), 747-762 (1955).

38. Archard, J. F., Kirk, M. T., "Lubrication At Point Contacts", Proc. Roy. Soc. (London) A, 261, 532-550 (1961).

39. Furey, M. J., "Metallic Contact and Friction Between Sliding Surfaces", ASLE Transactions 4, 1-11 (1961).

40. Yagoda, H., "Radioactive Measurements with Nuclear Emulsions", J. Wiley and Sons, Inc., New York, N. Y., (1948), 224.

41. Boyd, J. A., "Autoradiography in Biology and Medicine", Academic Press, New York, N. Y. (1955).

42. Klaus, E. E., Fenske, M. R., Tewksbury, E. J., "Fluids, Lubricants, Fuels and Related Materials", WADD Technical Report 55-30, Part 8 (1960).

43. Klaus, E. E., Fenske, M. R., "Fluids, Lubricants, Fuels and Related Materials", WADC Technical Report 55-30, Part 5 (1957) 11.

44. Mahoney, C. L., et. al., "Engine Oil Development," WADC Technical Report 57-177, Part 2 (1958).

45. Klaus, E. E., Pennsylvania State University, University Park, Pa., private communication.

46. Warren, B. E., Massachusetts Institute of Technology, Cambridge, Mass., private consultation.

47. General Electric XRD-5 Instruction Manual, Direction No. 12446.

48. Cullity, B. D., "Elements of X-Rav Diffraction," Addison-Wesley Pub. Co., Inc. (1956), Reading, Mass. 190-193.

ENCLOSURE I

SUBSURFACE CONTACT STRESSES CAUSED BY ELASTOHYDRODYNAMIC PRESSURES

ACCORDING TO DOWSON & HIGGINSON (21)

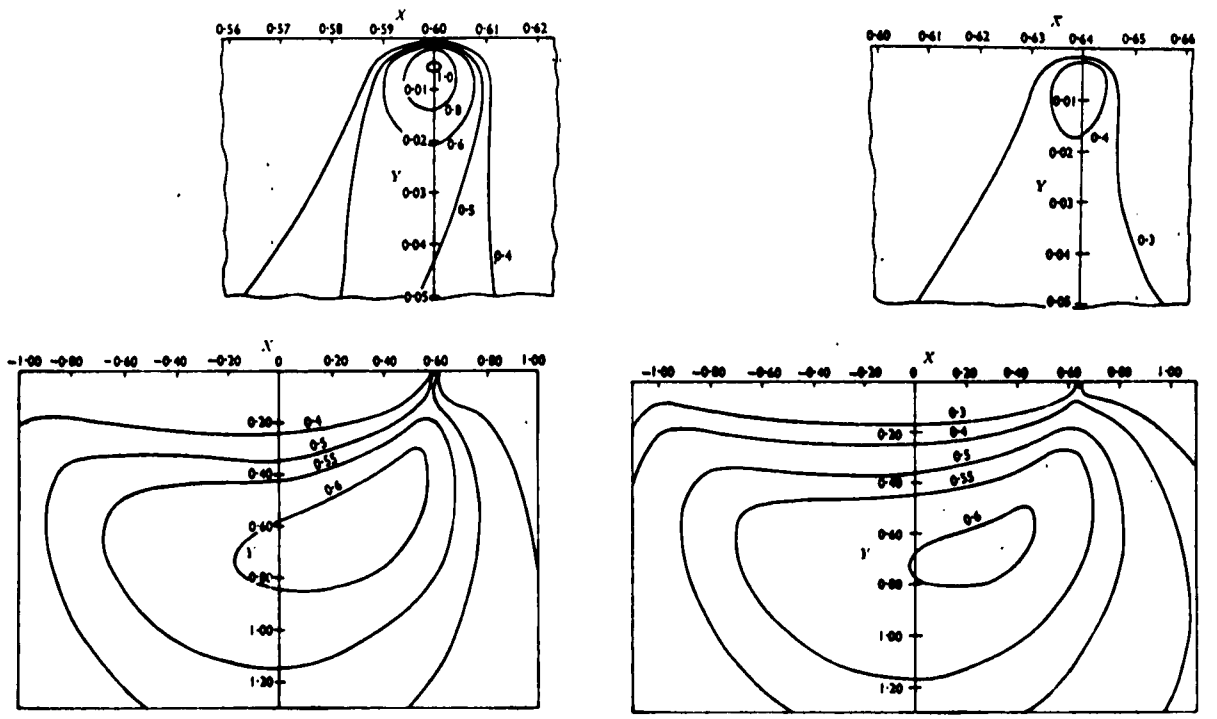

(a) $G = 5000$.

(b) $G = 2500$.

Contours of (maximum principal stress difference)/(maximum Hertzian pressure)

$W = 3 \times 10^{-5}$. $U = 10^{-11}$.

ENCLOSURE 2

TYPICAL PRESSURE DISTRIBUTION & FILM THICKNESS AS A FUNCTION OF ROLLER VELOCITY & CONTACT PRESSURE

FIG. A&B ACCORDING TO ARCHARD, GAIR & HIRST (22)

FIG. C ACCORDING TO BELL (25)

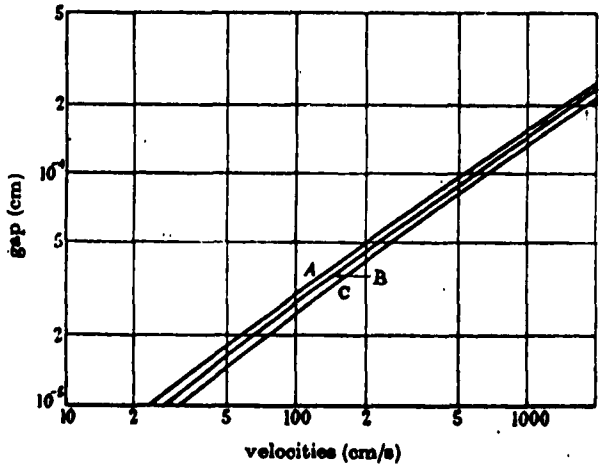

FIGURE a Width of oil film as a function of roller velocity and p_0.

η_0 = 0·4 P
p_0 = 2·5 tons/in.² (4 × 10⁸ dyn/cm²)
R = 1·9 cm (0·75 in.)
$1/\theta$ = 3·5 × 10¹³ dyn/cm³ (22500 tons/in.³)
A, p_0 = 4·8 × 10⁸ dyn/cm² (31 tons/in.².)
B, p_0 = 7·2 × 10⁸ dyn/cm² (46 tons/in.²)
C, p_0 = 9·6 × 10⁸ dyn/cm² (62 tons/in.²)

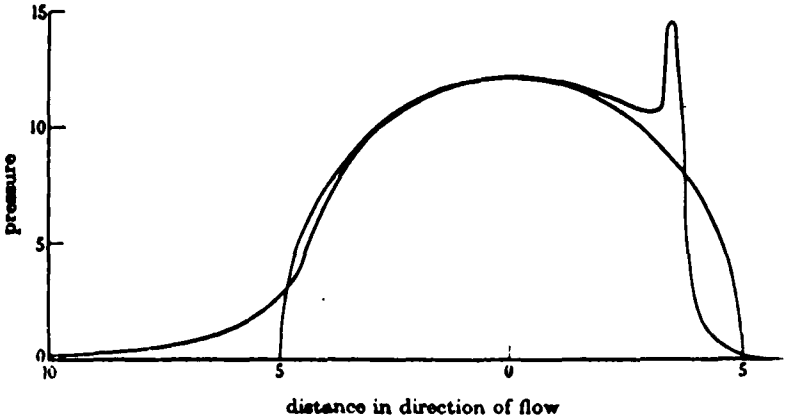

FIGURE b Pressure distribution.

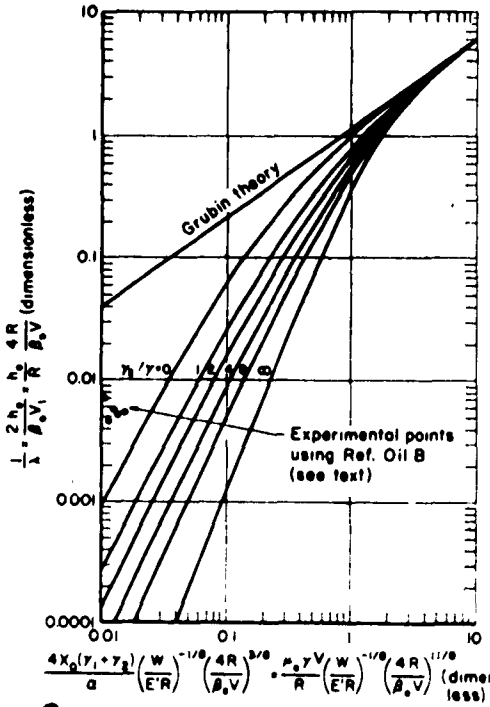

FIG. C Graph for finding film thickness of a Ree-Eyring lubricant between rolling cylinders.

ENCLOSURE 3

FOUR BALL TESTER CROSS SECTION

(SCALE : FULL)

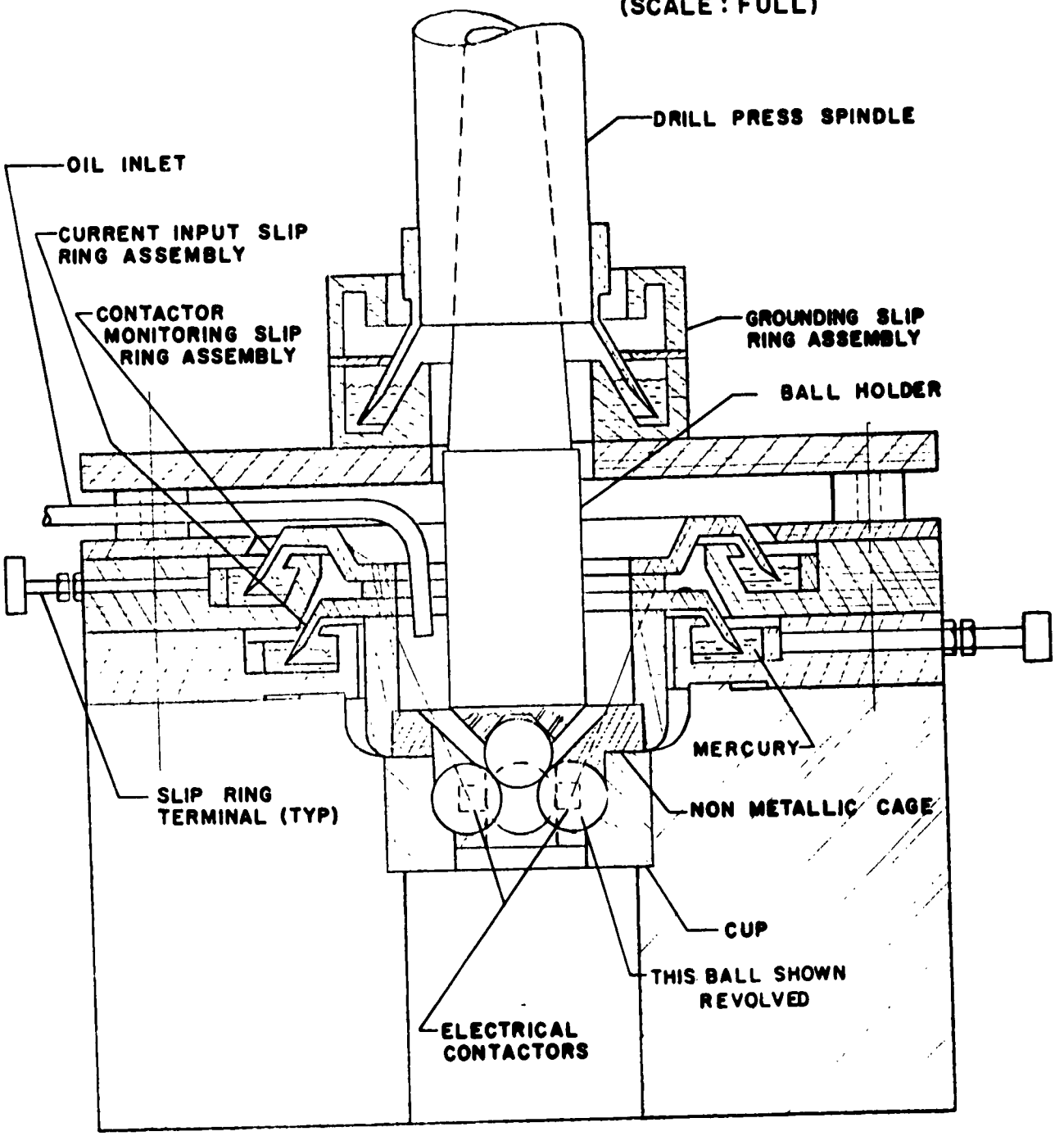

ENCLOSURE 4

PHOTOMICROGRAPHS OF ELECTRICAL CONTACTORS

(SHOWN ENLARGED ABOUT 13 TIMES)

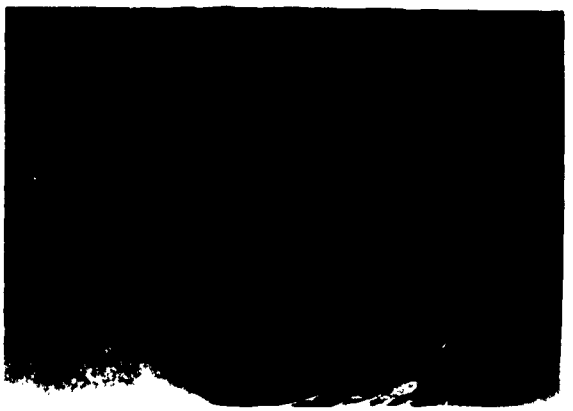

OBLIQUE VIEW OF CONTACTING SURFACE

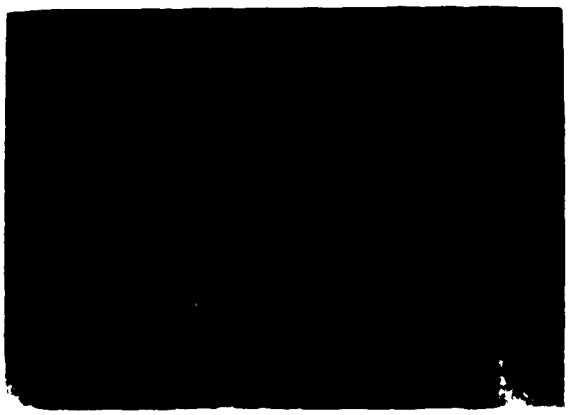

SIDE VIEW OF CONTACTOR

ENCLOSURE 5

SCHEMATIC OF FINAL ELECTRICAL CIRCUIT

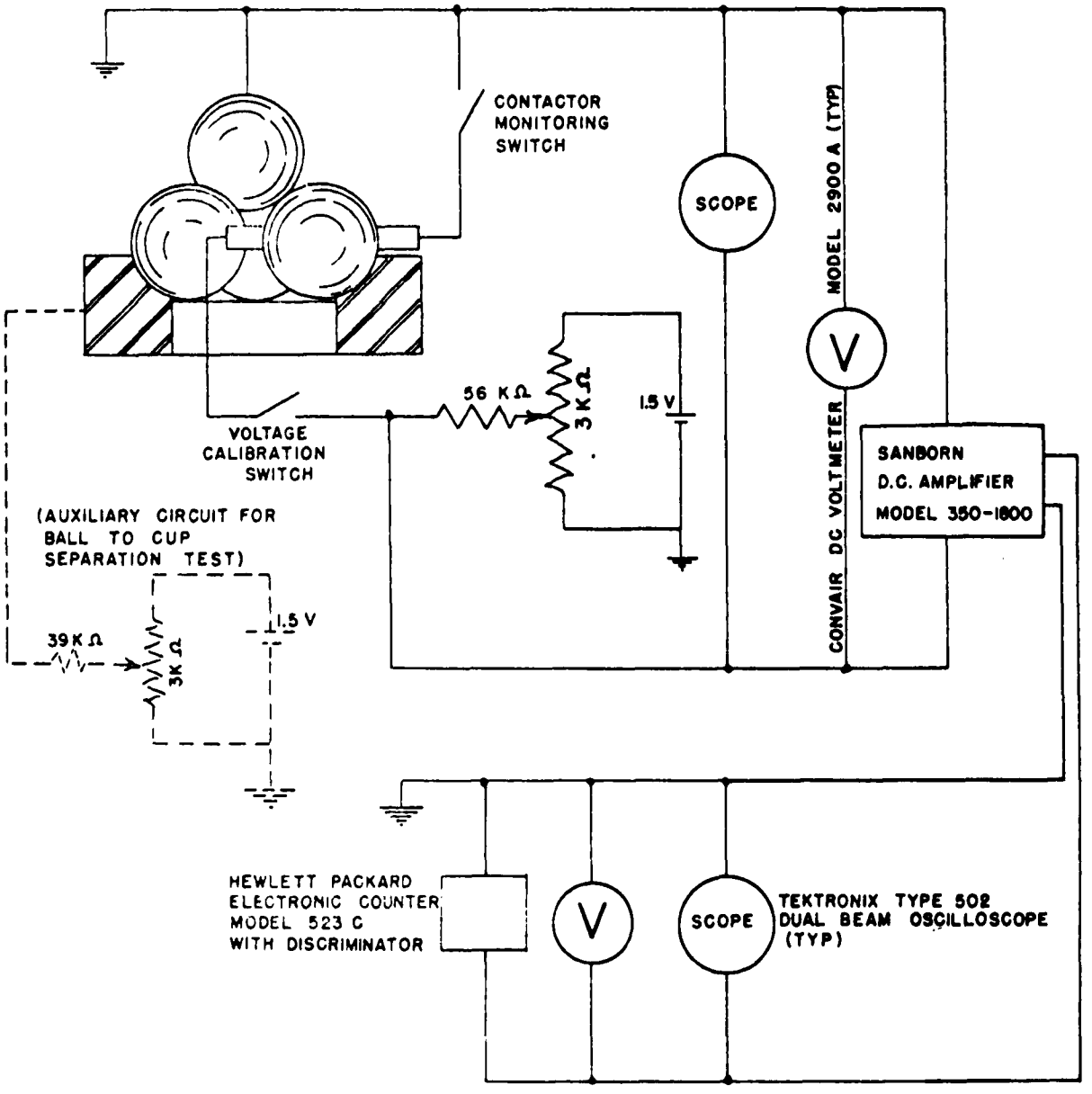

ENCLOSURE 6

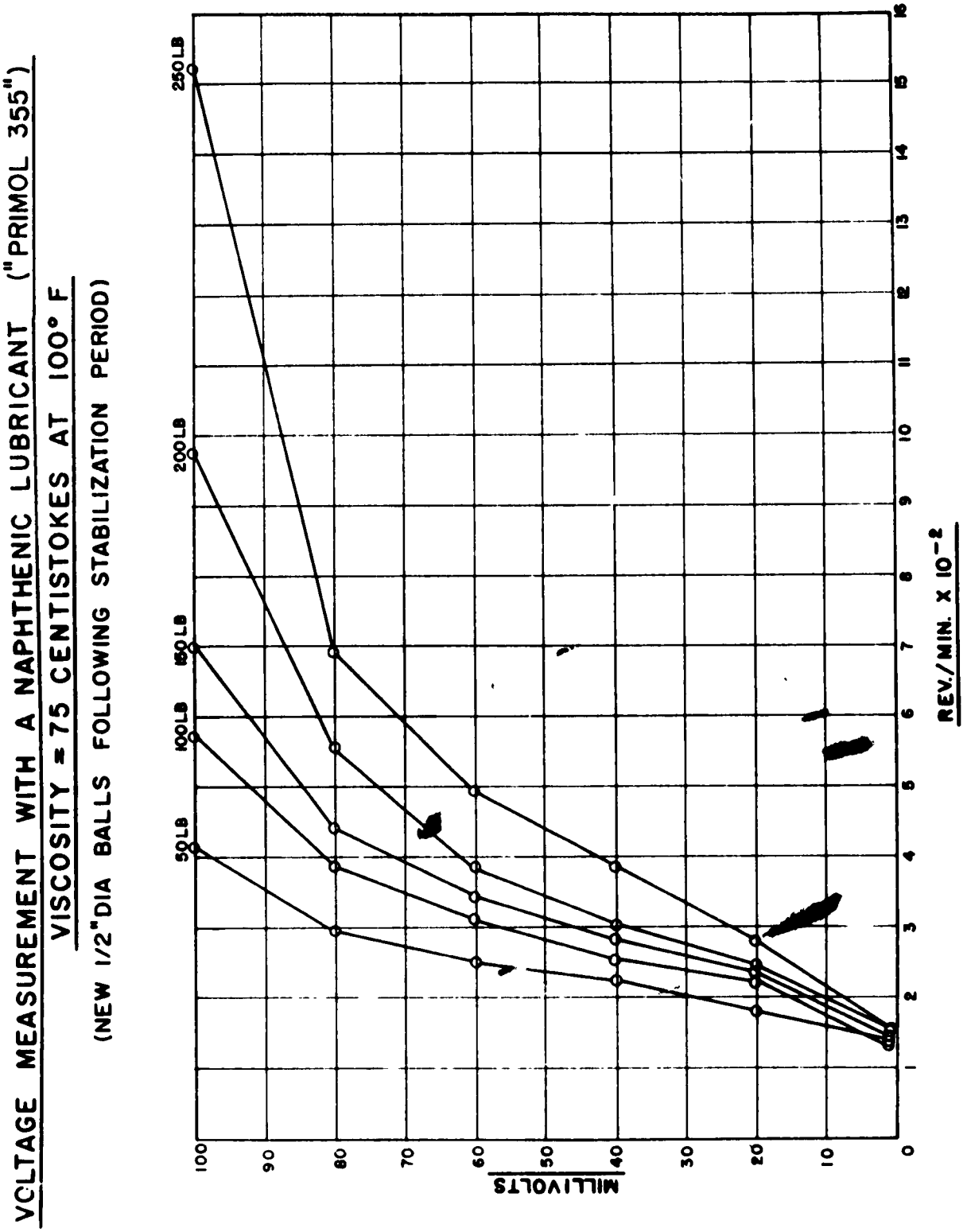
VOLTAGE MEASUREMENT WITH A NAPHTHENIC LUBRICANT ("PRIMOL 355")
VISCOSITY = 75 CENTISTOKES AT 100° F
(NEW 1/2" DIA BALLS FOLLOWING STABILIZATION PERIOD)
250 LB
200 LB
150 LB
100 LB
50 LB
100
90
80
70
60
50
40
30
20
10
0
MILLIVOLTS
REV./MIN. X 10⁻²

ENCLOSURE 7

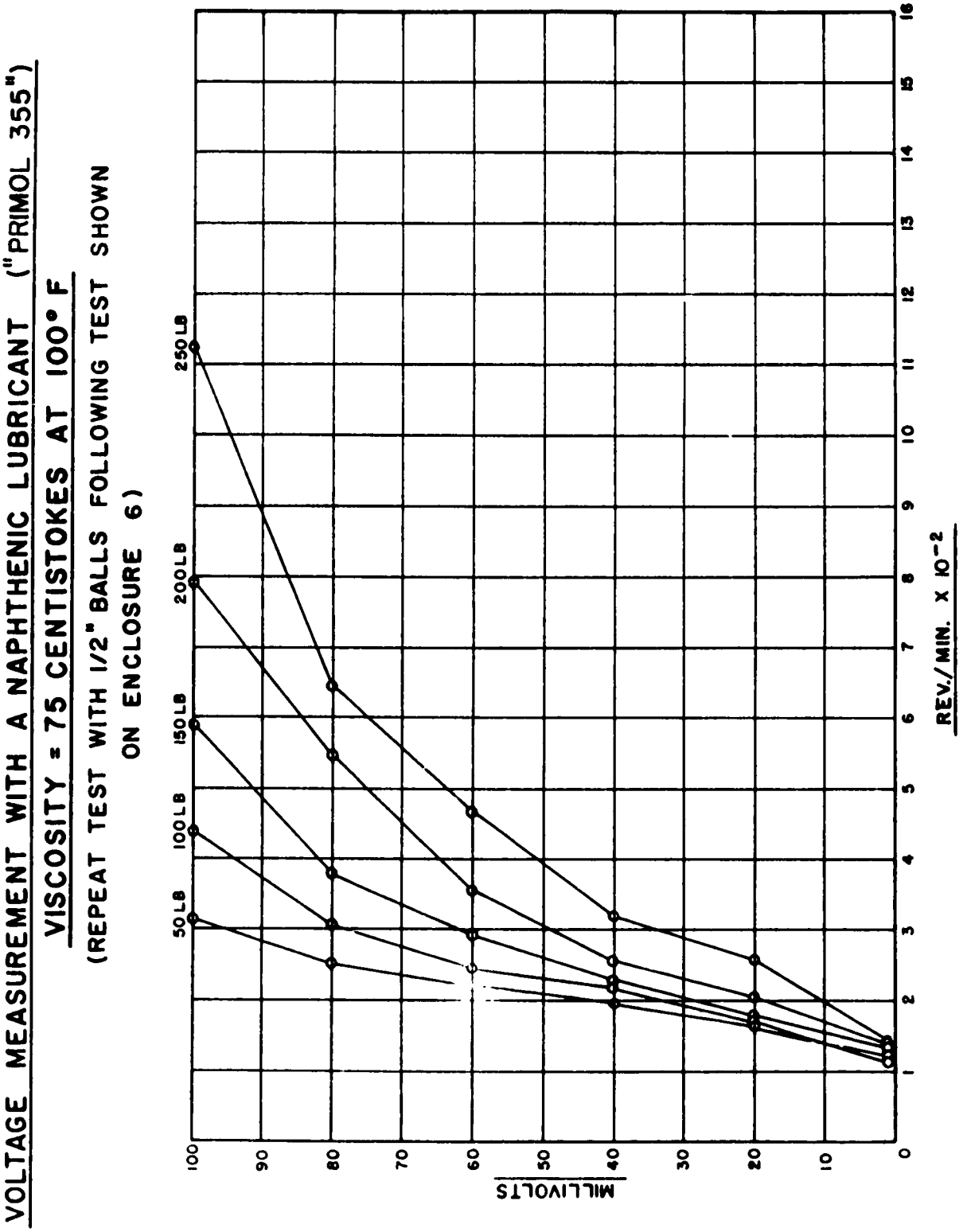
VOLTAGE MEASUREMENT WITH A NAPHTHENIC LUBRICANT ("PRIMOL 355")
VISCOSITY = 75 CENTISTOKES AT 100° F
(REPEAT TEST WITH 1/2" BALLS FOLLOWING TEST SHOWN ON ENCLOSURE 6)
250 LB
200 LB
150 LB
100 LB
50 LB
100
90
80
70
60
50
40
30
20
10
0
MILLIVOLTS
REV./MIN. X 10⁻²
1
2
3
4
5
6
7
8
9
10
11
12
13
14
15
16

ENCLOSURE 8

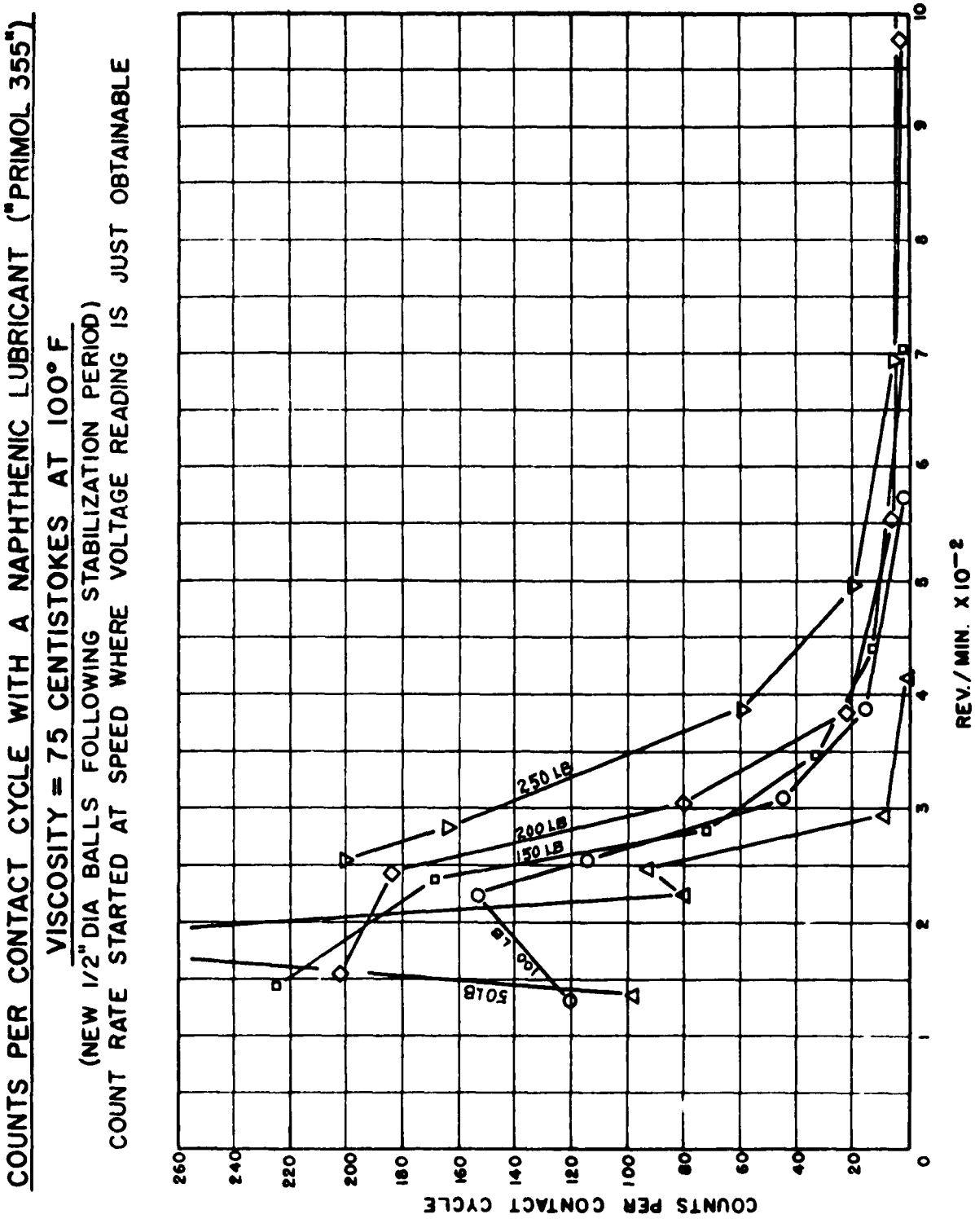
COUNTS PER CONTACT CYCLE WITH A NAPHTHENIC LUBRICANT ("PRIMOL 355")
VISCOSITY = 75 CENTISTOKES AT 100° F
(NEW 1/2" DIA BALLS FOLLOWING STABILIZATION PERIOD)
COUNT RATE STARTED AT SPEED WHERE VOLTAGE READING IS JUST OBTAINABLE
250 LB
200 LB
150 LB
100 LB
50 LB
COUNTS PER CONTACT CYCLE
260
240
220
200
180
160
140
120
100
80
60
40
20
0
REV./MIN. X10⁻²
10
9
8
7
6
5
4
3
2
1

ENCLOSURE 9

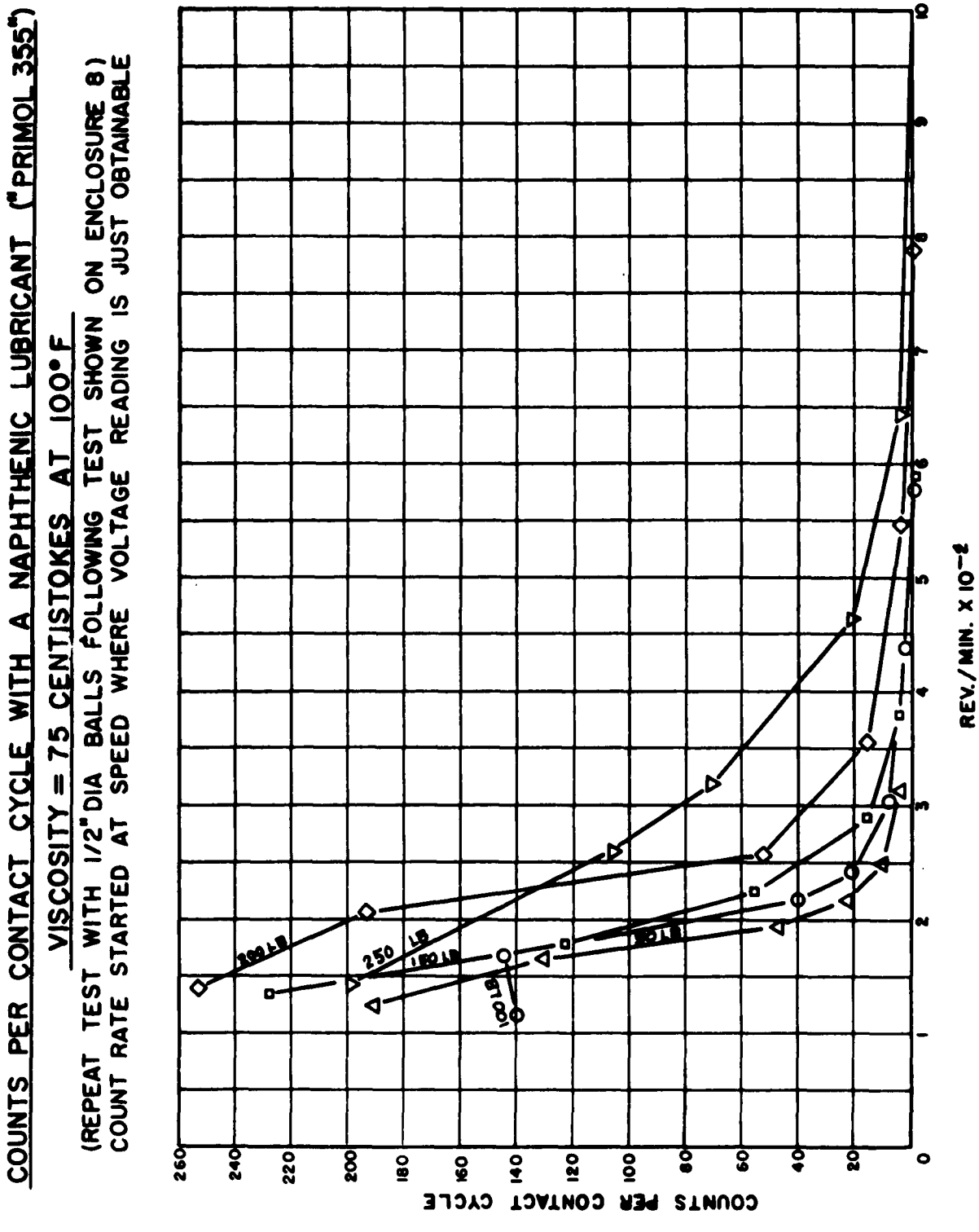
COUNTS PER CONTACT CYCLE WITH A NAPHTHENIC LUBRICANT ("PRIMOL 355")
VISCOSITY = 75 CENTISTOKES AT 100°F
(REPEAT TEST WITH 1/2" DIA BALLS FOLLOWING TEST SHOWN ON ENCLOSURE 8)
COUNT RATE STARTED AT SPEED WHERE VOLTAGE READING IS JUST OBTAINABLE
250 LB
200 LB
150 LB
100 LB
COUNTS PER CONTACT CYCLE
260
240
220
200
180
160
140
120
100
80
60
40
20
0
REV./MIN. X 10⁻²
0
1
2
3
4
5
6
7
8
9
10

ENCLOSURE 10

VOLTAGE MEASUREMENTS WITH A WHITE MINERAL OIL

VISCOSITY = 80 CENTISTOKES AT 100°F
(PRELIMINARY TESTS WITH NEW 1/2" DIA BALLS)

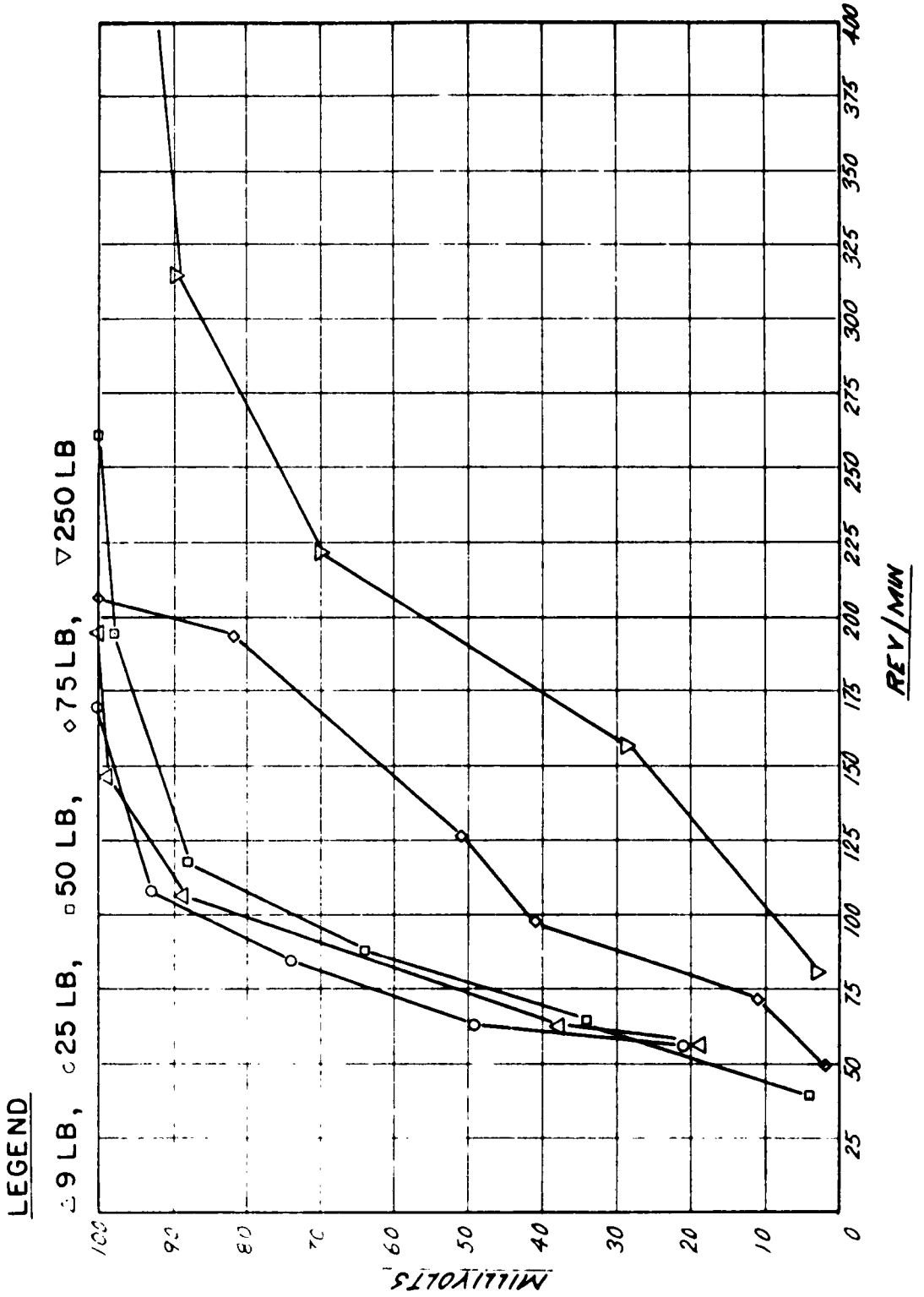

ENCLOSURE II

VOLTAGE MEASUREMENTS WITH A POLYOLEFIN LUBRICANT (MLO 7584)

VISCOSITY = 117 CENTISTOKES AT 100°F
(PRELIMINARY TESTS WITH NEW 1/2" DIA BALLS)

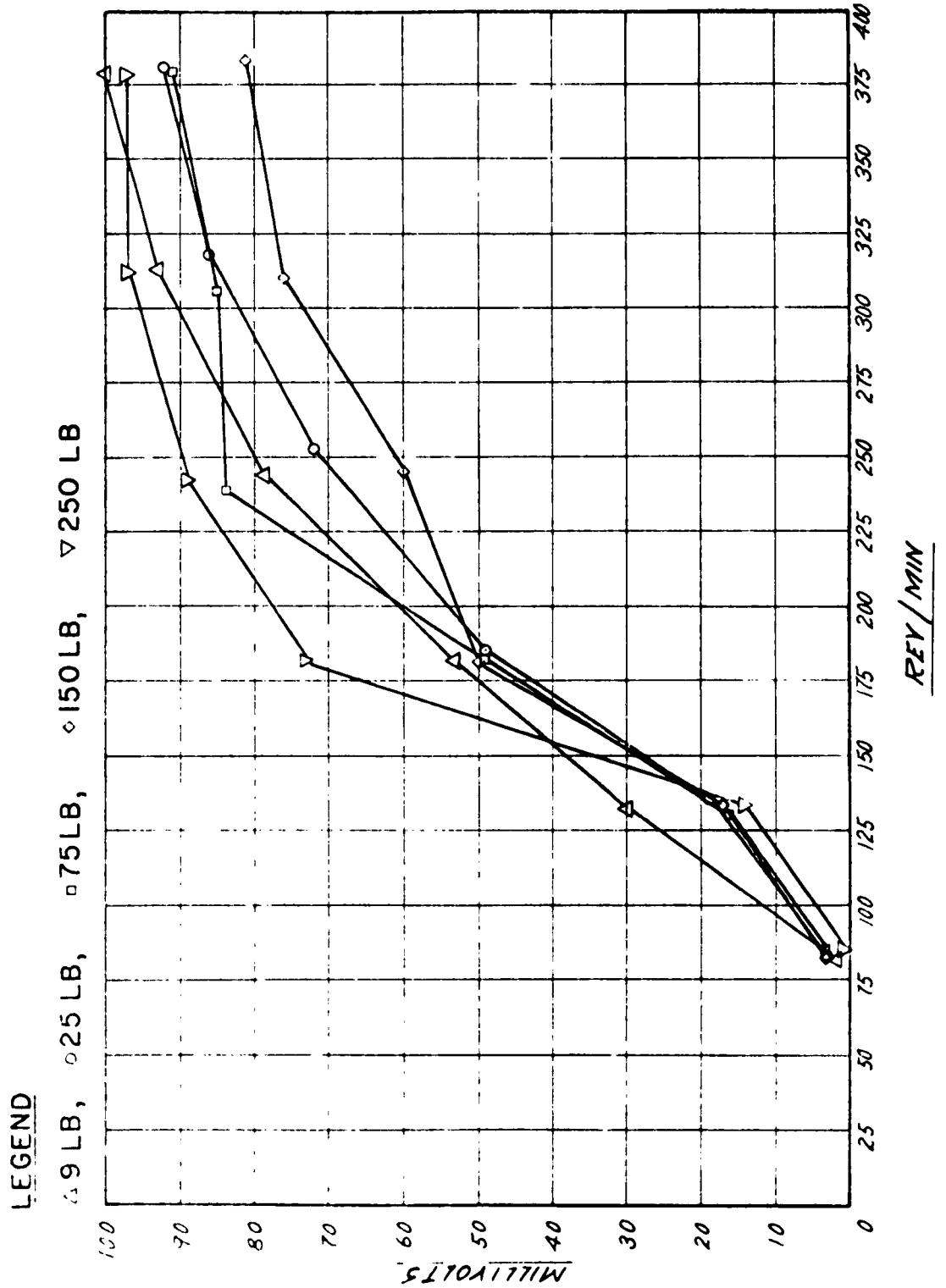

ENCLOSURE 12

VOLTAGE MEASUREMENTS WITH A DIESTER LUBRICANT (MLO 7593)

VISCOSITY = 24 CENTISTOKES AT 100°F

(PRELIMINARY TESTS WITH NEW 1/2" DIA BALLS)

LEGEND

△9LB, ○25LB, □75LB, ◇150LB, ▽250LB

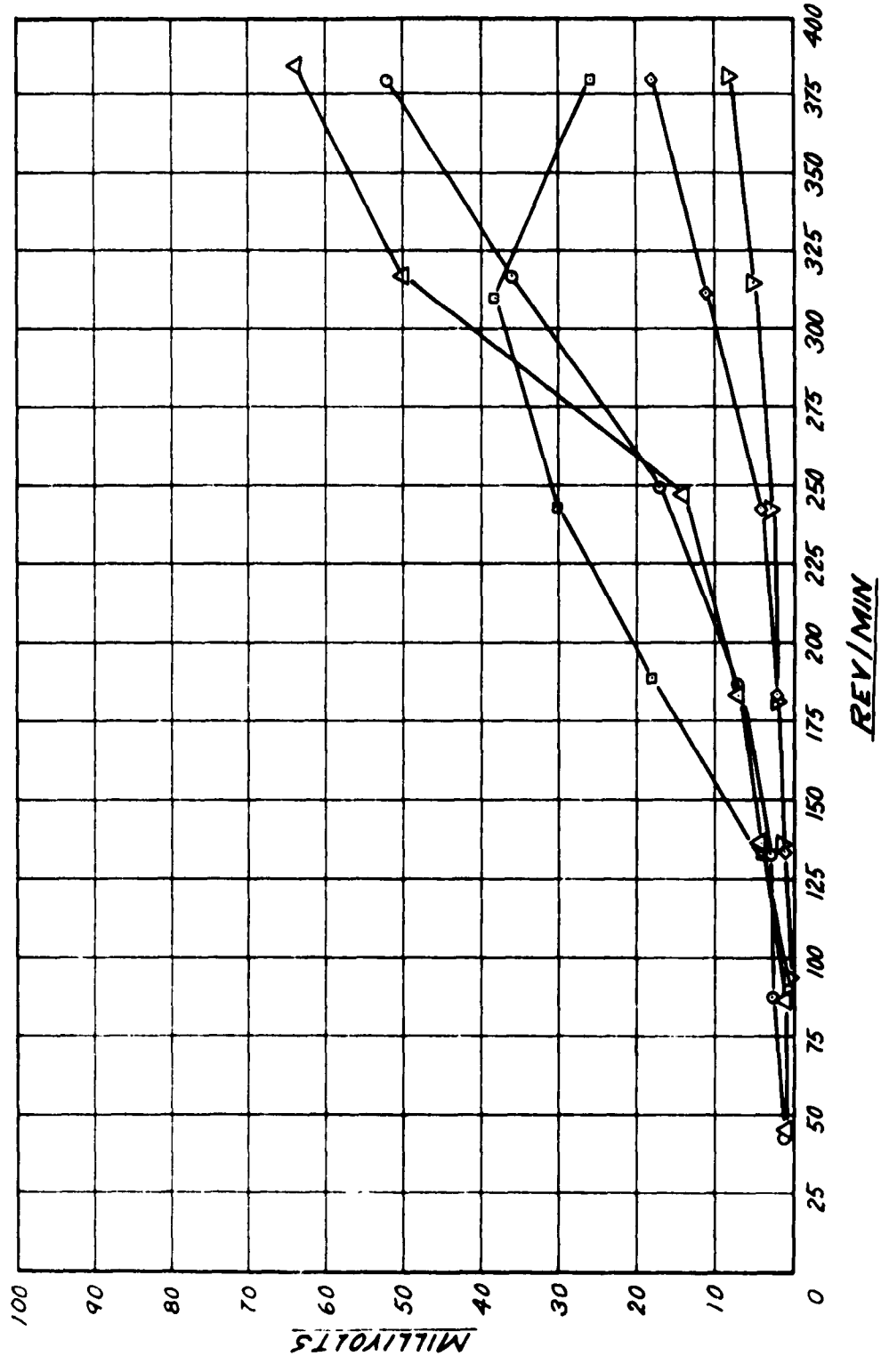

ENCLOSURE 13

MAXIMUM CONTACT STRESS FOR 1/2" DIAMETER BALLS AS A FUNCTION OF APPLIED BEARING LOAD WITH A 40° CONTACT ANGLE

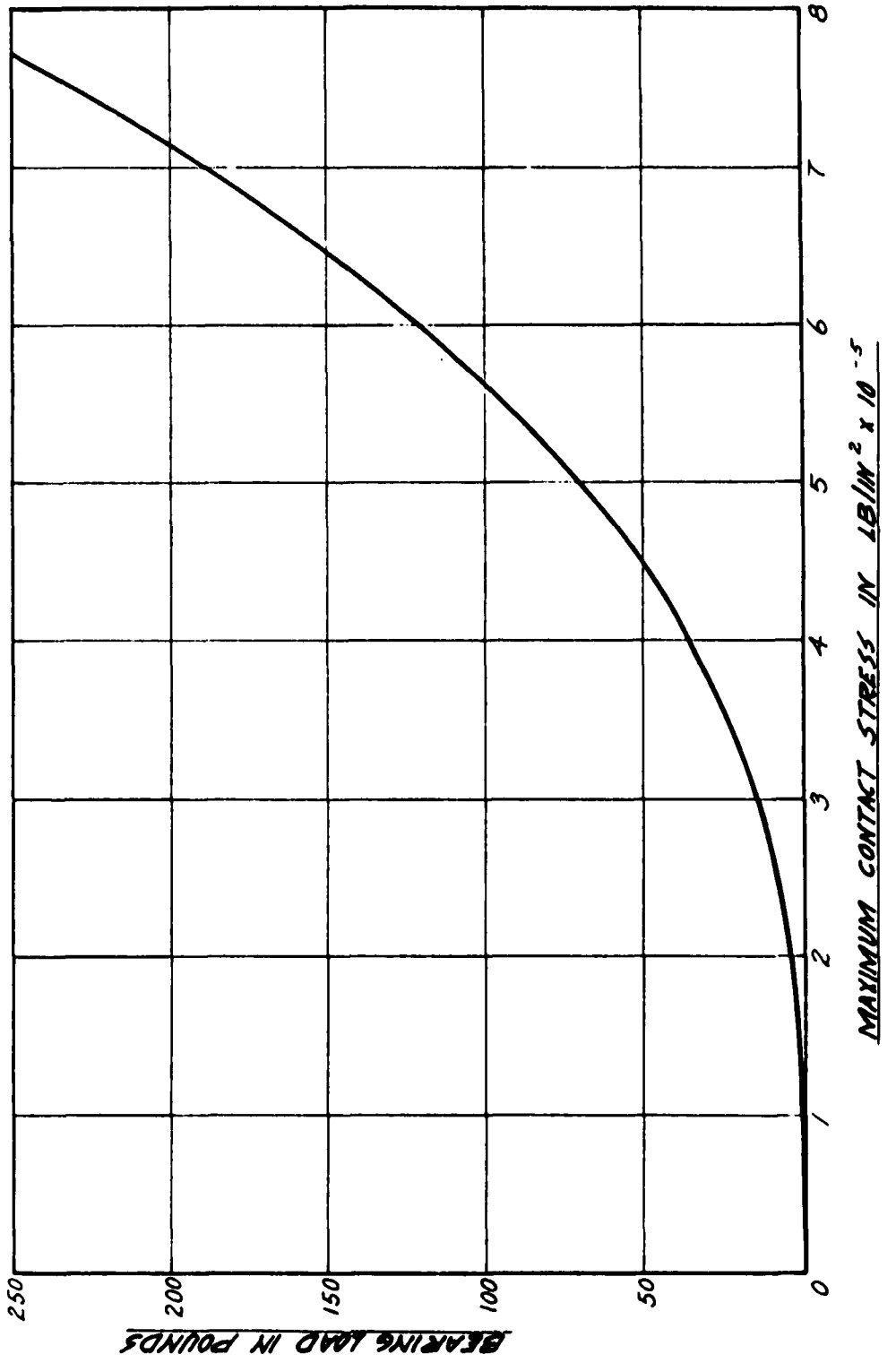

ENCLOSURE 14

TYPICAL OSCILLOSCOPE TRACES OF VARIOUS INDICATED SEPARATION CONDITIONS

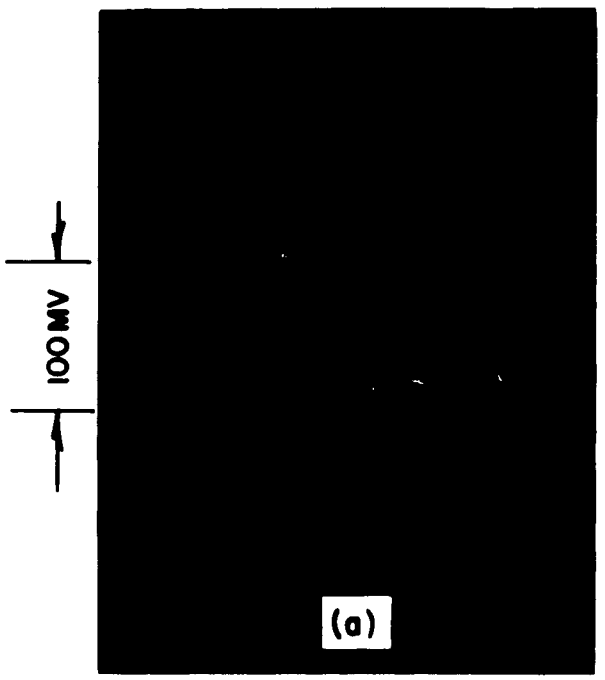

HORIZONTAL SWEEP 5 MILLI-SEC/CM
VOLTAGE PARTIALLY RISING FROM SHORTED CONDITION

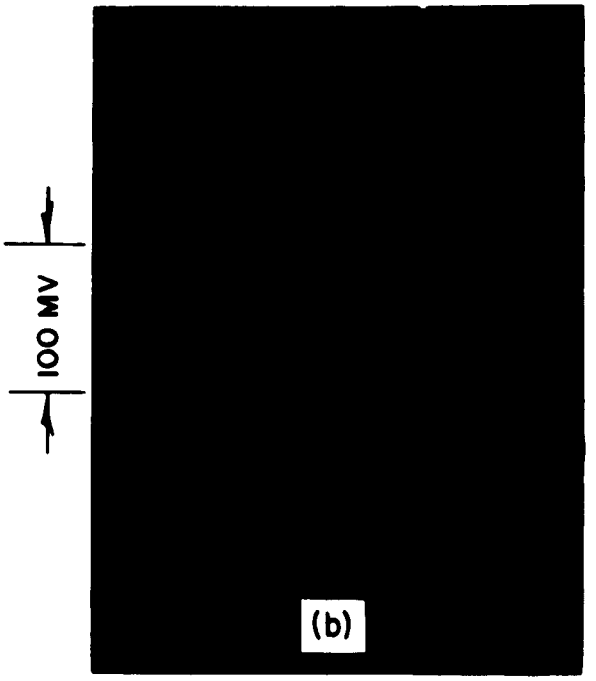

HORIZONTAL SWEEP 5 MILLI-SEC/CM
INDICATED COMPLETE SEPARATIONS AND SHORTS WITH INTERMEDIATE LEVELS

HORIZONTAL SWEEP 5 MILLI-SEC/CM
VOLTAGE DROPPING FROM INDICATED SEPARATION LEVEL

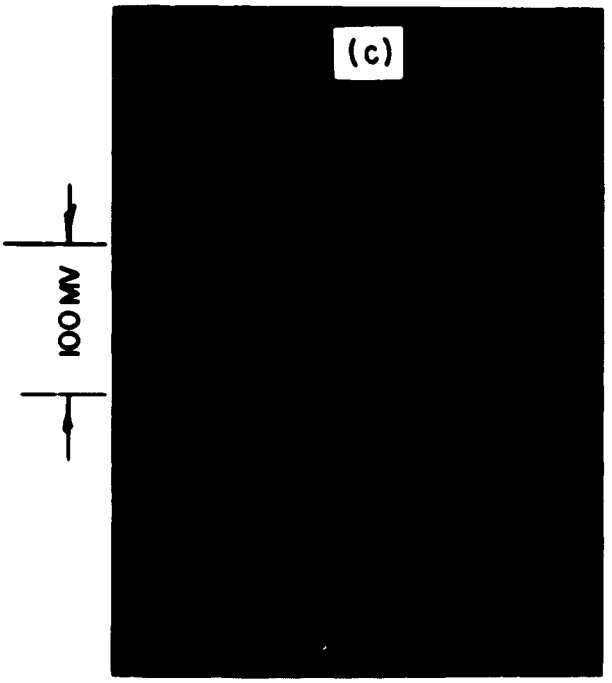

HORIZONTAL SWEEP 0.1 MILLI-SEC/CM
EXPANDED VIEW OF AN INTERMEDIATE VOLTAGE LEVEL

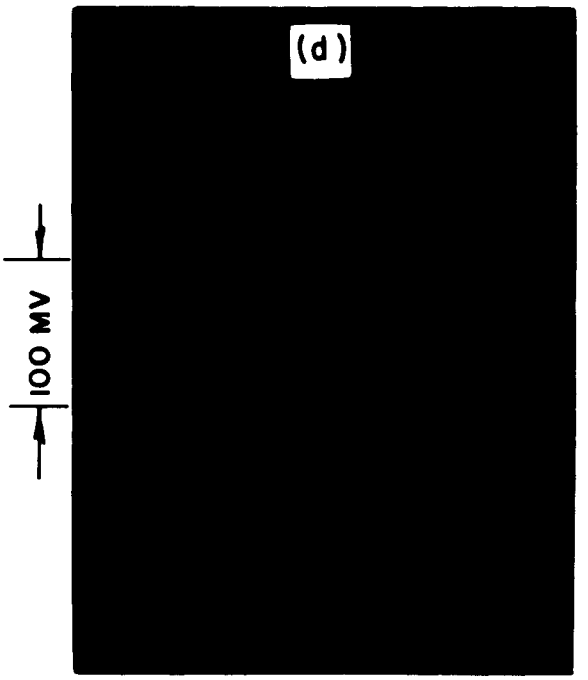

ENCLOSURE 15

AL62T004

VOLTAGE RISE AS A FUNCTION OF RUNNING TIME

TEST CONDITIONS

◇ NEW SET OF BALLS WITH SURFACE ROUGHNESS LESS THAN ONE MICRO-INCH, 50 LB. LOAD @ 770 REV/MIN., NAPTHENIC OIL (MLO 7277).

▽ NEW SET OF BALLS WITH SURFACE ROUGHNESS LESS THAN ONE MICRO-INCH, 50 LB. LOAD @ 384 REV/MIN, NAPTHENIC OIL (MLO 7558).

▫ NEW SET OF BALLS WITH SURFACE ROUGHNESS LESS THAN ONE MICRO-INCH, 50 LB. LOAD @ 384 REV./MIN., ESTERBASE OIL (MLO-7593).

△ NEW SET OF BALLS WITH SURFACE ROUGHNESS LESS THAN ONE MICRO-INCH, 50 LB. LOAD @ 212 REV/MIN, MINERAL OIL ("NUJOL").

○ NEW SET OF ETCHED BALLS WITH SURFACE ROUGHNESS OF ABOUT THREE MICRO-INCH, 50 LB. LOAD @ 384 REV/MIN, ESTERBASE OIL (MLO-7593). FOUR HOURS RUNNING TIME WAS ALLOWED BEFORE THE READINGS SHOWN WERE TAKEN.

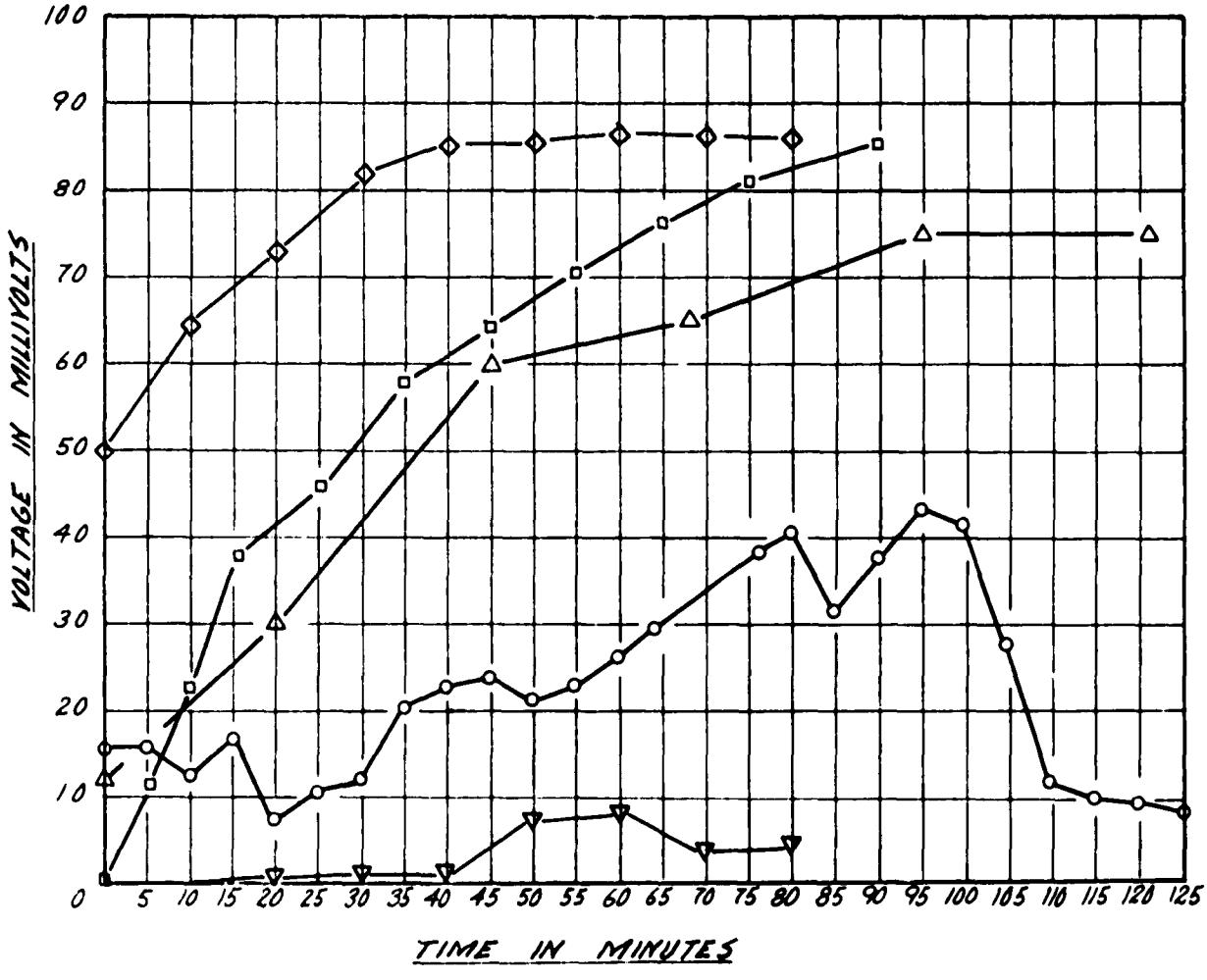

ENCLOSURE 16

TALYROND & TALYSURF TRACES OF 1/2" DIA BALL AFTER TEST RUNS

14 a

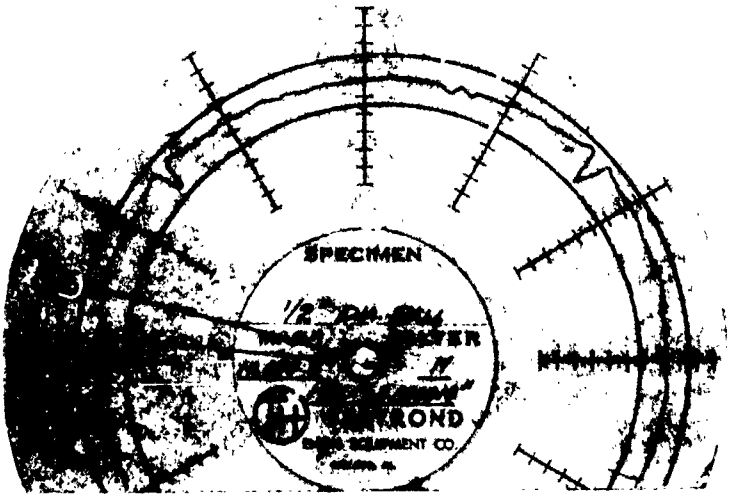

14 b TALYSURF TRACES TAKEN 90° APART ACROSS BALL TRACK

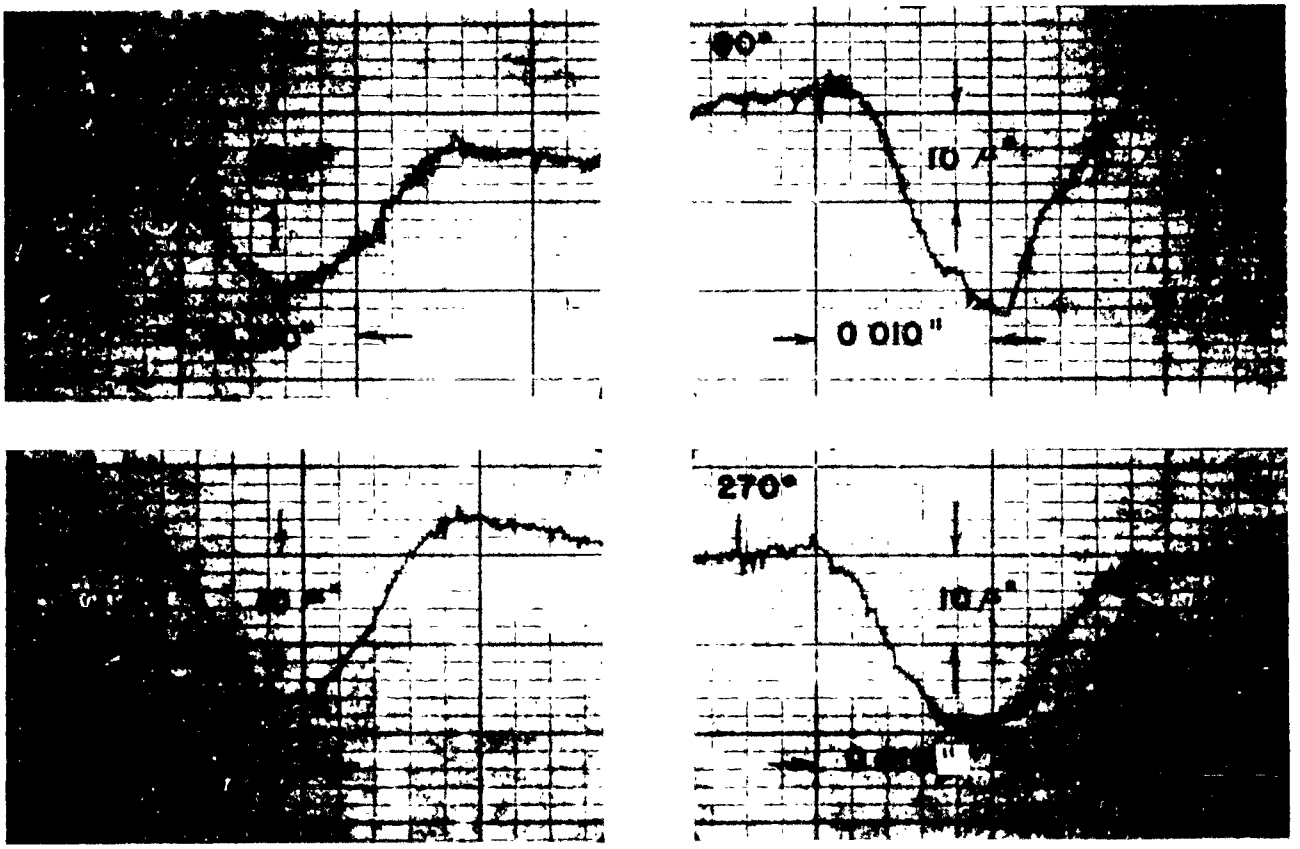

ENCLOSURE 17a

PHOTOMICROGRAPHS OF UPPER TEST BALL SHOWING TRACKING EFFECTS

SKETCH OF UPPER BALL SHOWING THE ORIENTATION & APPROXIMATE FIELD OF VIEW OF THE PHOTOMICROGRAPHS SHOWN ON ENCLOSURES 17a & 17b

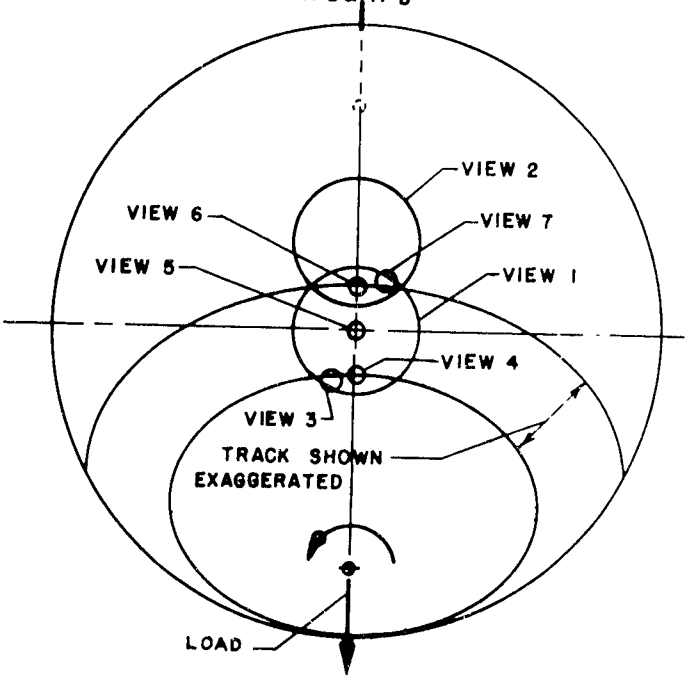

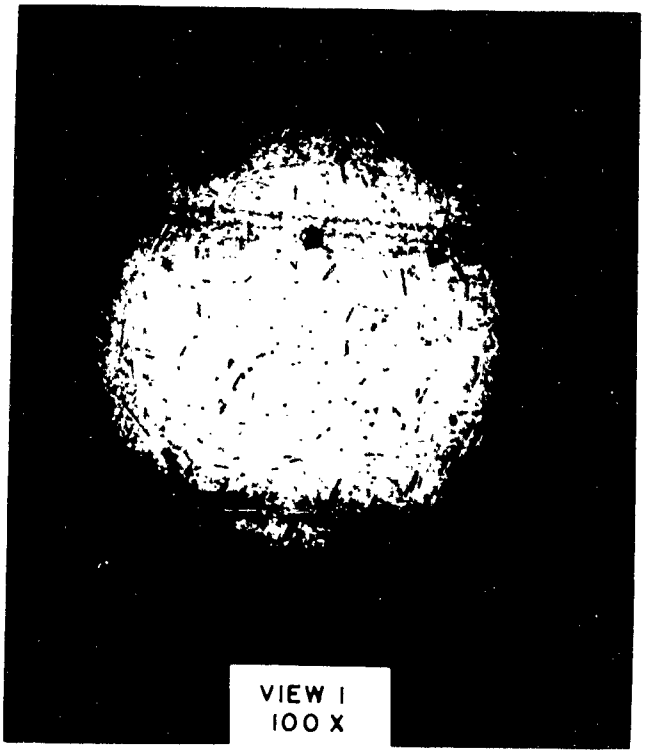

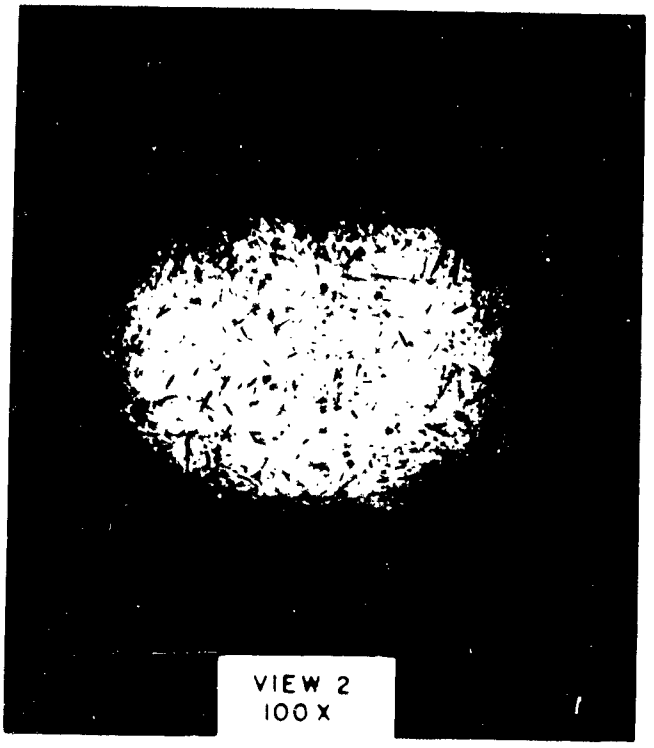

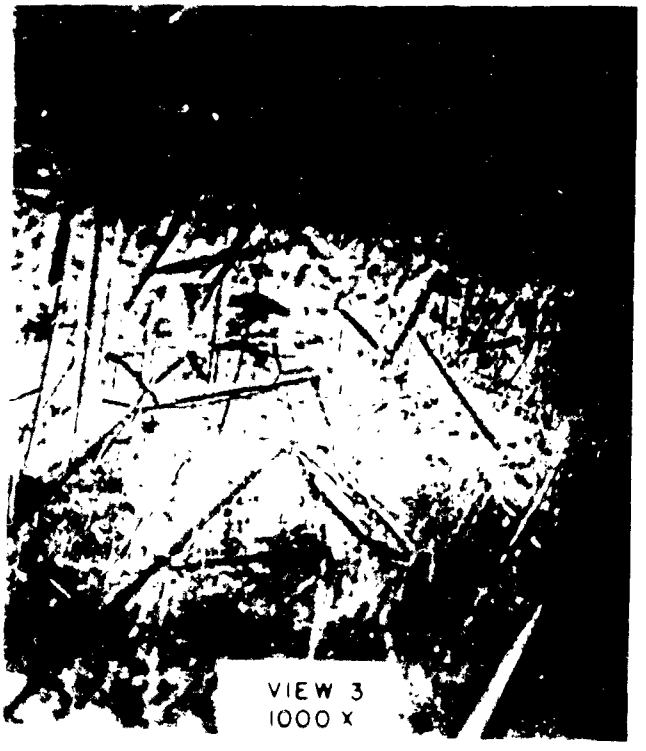

ENCLOSURE 17b

PHOTOMICROGRAPHS OF UPPER TEST BALL SHOWING TRACKING EFFECTS

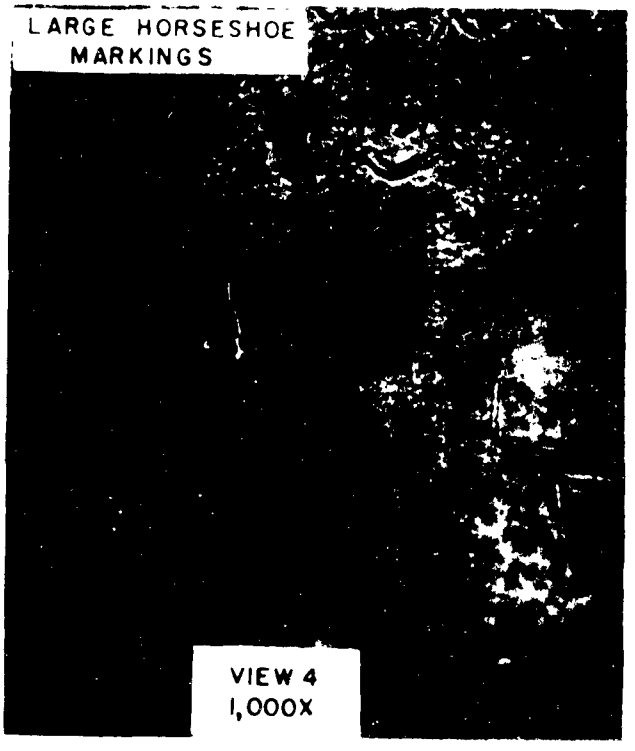

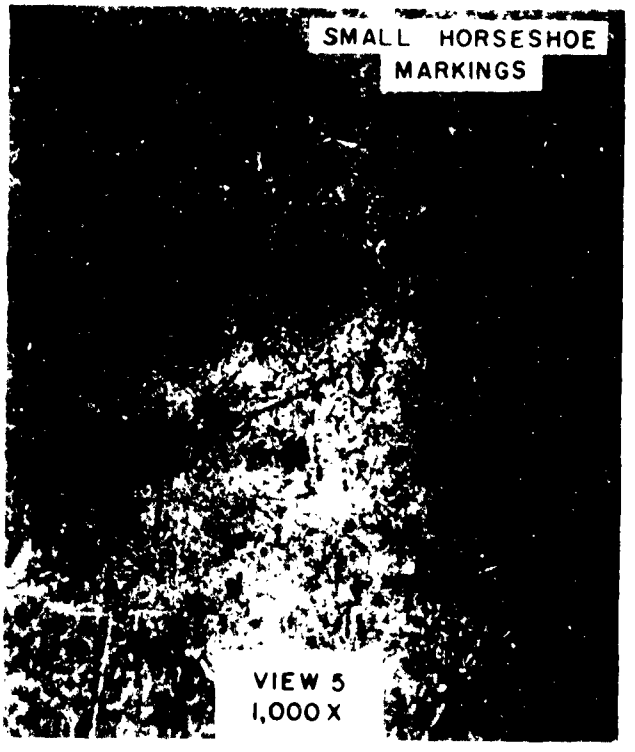

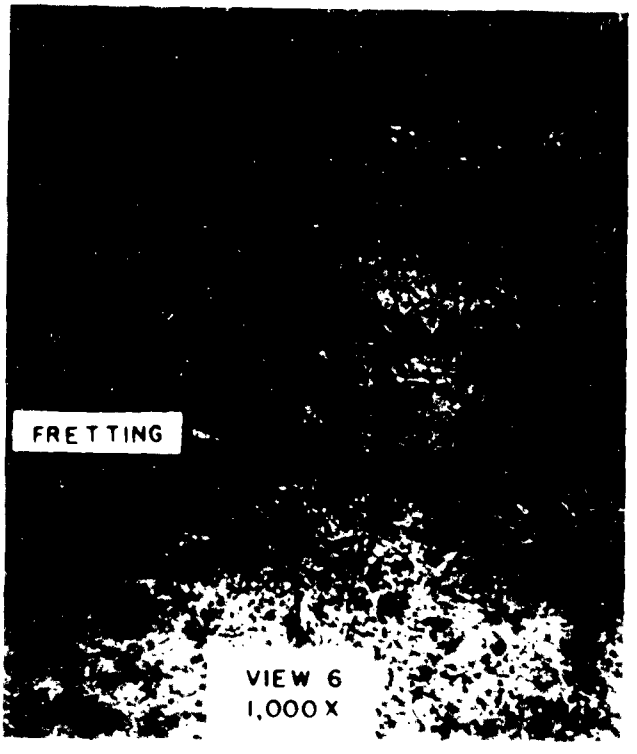

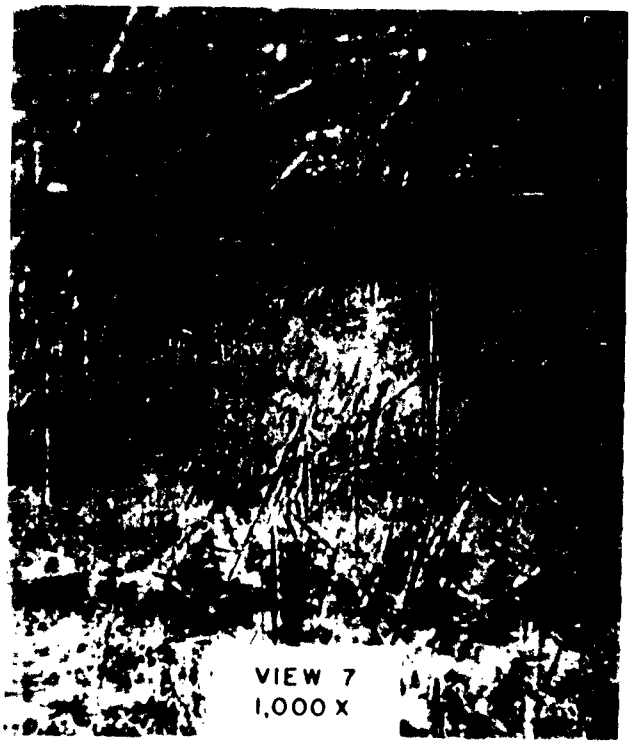

COMPOSITION OF HIGH TEMPERATURE LUBRICANTS

IDENTIFICATION	BASE STOCK	ANTIOXIDANTS (IN WEIGHT PERCENT)	E. P. ADDITIVIES (IN WEIGHT PERCENT)	FOAM INHIBITORS IN PARTS PER MILLION (PPM) NOTE 1
MLO-7593	DI-2-ETHYLHEXYLSEBACATE	PHENOTHIAZINE 1.0 PHENYL-ALPHA-NAPHTHYLAMINE (PAN) 2.0	ACRYLOID - 966 5.0 NOTE 2	10
MLO-7584	POLYISOBUTENE (SIMILAR TO STD. OF INDIANA INDOPOL L-50)	—	—	10
MLO-7558	AN ACID TREATED NAPHTHENIC WHITE OIL 25.9% ISO PARAFFINS 30.1% ONE RING NAPHTHENES 20.1% TWO RING NAPHTHENES 23.9% THREE PLUS RING NAPHTHENES	—	—	—
MLO-7582	(AN ACID TREATED NAPHTHENIC WHITE OIL (ESSO PRIMOL 355)	PAN 1.0	--	10
MLO-7277	5.9% ISO PARAFFINS 23.8% ONE RING NAPHTHENES	PAN 1.0	TRICRESYLPHOSPHATE 1.0	10
MLO-7451	26.2% TWO RING NAPHTHENES 34.7% THREE PLUS RING NAPHTHENES	PAN 1.0	DI-ISOPROPYLACID - PHOSPHITE 0.5	10
MLO-7583	RAFFINATE EXTRACT OF PROPANE REFINED PARAFFINIC LUBE OIL STOCK (KENDALL RESIN)	PARANOX 441 0.5 NOTE 3	—	10
MLO-7503	MIXED 5-RING POLYPHENYL-ETHER (MONSANTO OS-124)	—	—	—
MLO-7017	VERSILUBE F-50 (GENERAL ELECTRIC Co.) - AN IMPROVED LUBRICITY SILICONE OIL	—	—	—

NOTE 1: FOAM INHIBITOR USED IS A METHYLSILICONE IN A HYDROCARBON CARRIER.

NOTE 2: WHILE DISPERSANT METHACRYLATE POLYMERS SUCH AS ACRYLOID 966 ARE NOT CONSIDERED TO BE E. P. AGENTS, THE INCREASE IN VISCOSITY FROM ABOUT 12 CS AT 100°F FOR THE BASE OIL TO 24.4 CS FOR THE ACRYLOID CONTAINING FORMULATION INCREASES CONSIDERABLY THE LOAD - CARRYING CAPABILITY OF DI-2-ETHYLHEXYLSEBACATE AT LEAST AS EVIDENCED IN GEAR TESTS.

NOTE 3: PARANOX 441 IS ADDED TO INCREASE THE STORAGE LIFE OF MLO-7583 AND HAS LITTLE OR NO EFFECT ON THE HIGH-TEMPERATURE OXIDATION STABILITY OF THE FORMULATION.

VISCOSITY-TEMPERATURE PROPERTIES

	Kinematic Viscosity at °F, cs									VI (ASTM D-567)	ASTM Slope	Pour Pt, °F	Flash Pt, °F	Fire Pt, °F	Neut. No.
	700	500	400	210	100	30	0	-40	-65						
MLO-7593	--	--	--	--	24.4	--	--	--	--	--	--	-75	476	550	0.1
MLO-7584	--	--	2.08	11.1	116	--	14,500	--	--	87	0.727	-25	325	--	0.1
MLO-7558	--	0.87	--	4.34	23.21	--	--	11,810	102,300	101	--	-70	400	460	0.0
MLO-{7562, 7277, 7451}	0.6	1.1	--	8.4	79.2	1500	10,000	--	--	74	0.759	-30	445	495	0.0
MLO-7583	--	--	9.90	131.5	3836	--	--	--	--	--	--	+40	550	620	0.1
MLO-7503	0.65	1.2	2.1	13.1	365	--	--	--	--	-80	--	+40	550	660	0.1
MLO-7017	2.2	4.5	--	21.0	55.9	--	287	934	2,300	--	0.315	-100	550	640	--

ENCLOSURE 20

AL621004

VISCOSITY -PRESSURE RELATIONSHIPS (PRL VISCOMETER)

	Atm. Visc. at 100°F (cs)	Viscosity Index	ASTM Slope	Centistoke Viscosity (Gas Free) at 100°F 200	500	1000 PSIG	Pressure Coefficient % change/100 PSIG Appl. Press. 0-200	0-500	0-1000 PSIG	Centistoke Viscosity at 100°F and 1000 PSIG, Gas Saturated
MLO-7593 (Data for Base Stock)	12.6	155	0.701	13.0	13.6	14.9	1.59	1.59	1.83	13.0
MLO-{7582 7277 7451	73.5	74	0.774	—	83.3	94.8	—	2.66	2.90	—
MLO-7583	3990	108	0.579	4230	4610	5280	3.01	3.11	3.24	3800
MLO-7503	369	-80	0.893	393	434	511	3.25	3.52	3.85	422
MLO-7017	55.9	164	0.323	58.1	61.6	67.8	1.97	2.04	2.13	49.4

DENSITY - TEMPERATURE RELATIONSHIPS

	0°F	100°F	200°F	300°F	400°F	500°F	600°F
MLO-7593 (BASE FLUID DATA)	--	0.901	0.862	0.823	0.783	0.741	--
MLO-7584	--	0.837	0.805	0.757	0.732	0.695	--
MLO-7277	0.908	0.873	0.838	0.802	0.768	0.732	--
MLO-7583	--	0.895	0.860	0.824	0.789	0.756	--
MLO-7503	--	1.187	1.148	1.100	1.057	1.013	0.971
MLO-7017	--	1.010	0.962	0.915	0.868	0.821	--

COEFFICIENT OF EXPANSION, 10^{-4} cc/cc °F

	0°F	100°F	200°F	300°F	400°F	500°F	600°F	700°F
MLO-7277	4.0	4.2	4.4	4.5	4.9	--	--	--
MLO-7583	--	3.3	3.4	3.5	3.8	4.2	4.7	5.3

THERMAL CONDUCTIVITY, BTU/HR FT °F

	°F	100°F	200°F	300°F	400°F	500°F
MLO-7598	--	0.0870	0.0861	0.0855	0.0849	0.0843
MLO-7584	--	0.0713	0.0713	0.0714	0.0719	0.0725
MLO-7277	0.0775	0.0732	0.0729	0.0705	0.0682	0.0659
MLO-7503	--	0.0768	0.0753	0.0733	0.0715	0.0695
MLO-7017	--	0.0895	0.0874	0.0861	0.0859	0.0858

SPECIFIC HEAT, BTU/LB °F

	°F	100°F	200°F	300°F	400°F	500°F	600°F	700°F
MLO-7277	0.424	0.471	0.519	0.566	0.615	0.660	--	--
MLO-7503	--	0.368	0.400	0.432	0.465	0.496	0.528	0.560

VAPOR PRESSURE, MM HG

	100°F	300°F	400°F	500°F	600°F	700°F	800°F
MLO-7277	--	0.1	2.0	17	--	--	--
MLO-7503	--	--	--	0.7	5.3	26	103
MLO-7017	6	22	40	64	--	--	--

EVAPORATION RATES AT 400°F; AIR FLOW: 2 LITERS/MINUTE TEST TIME: 6.5 HOURS

(MIL-L-7808 TEST METHOD)

	PERCENT WEIGHT LOSS
MLO-7593	16.
MLO-7584	67
MLO-7582	14.1
MLO-7277	15.2
MLO-7503	0.6
MLO-7017	1.1

ENCLOSURE 25

AL62T004

ELECTRICAL PROPERTIES AT 25° AND 100°C

	Dielectric Constant				Resistivity ohm-cm	Power Factor			
	60 cycle	1KC	10KC	100KC	at 500 VDC	60 cycle	1KC	10KC	100KC
MLO-7503 @25°C	4.47	4.47	4.47	4.47	7400 x 10^9	0.05%	0.01%	0.025%	0.22%
@100°C	3.89	3.89	3.88	3.88	2800 x 10^9	2.03%	0.09%	0.01%	0.01%

THERMAL STABILITY TESTS

TEST CONDUCTED IN NITROGEN ATMOSPHERE

	Test Temp. (°F)	Test Time (Hrs.)	In Glass with Metal Catalysts: $ Vis. Change	Neut. No. Increase	Insolubles ($)	In Steel Vessel: $ Vis. Change	Neut. No. Increase	Insolubles ($)
MLO-7593	600	6	-12	15	—	—	—	—
	650	6	Solid	125	100	—	—	—
MLO-7584	600	6	-12	0	None	-63	0	None
MLO-7582	700	6	-44	0	None	-45	0	None
MLO-7277	700	6	-44	0	None	-46	0	None
MLO-7583	600	6	-26	0	None	-22	0	None
	700	6	-92	0	None	—	—	—
	700	2	—	—	—	-98	0	None
MLO-7503	700	6	0	0.1	None	—	—	—
MLO-7017	700	6	-21	13.6	None	—	—	—

OXIDATION - CORROSION STABILITY (IN PRESENCE OF FE, AL AND CU CATALYSTS)

	Test Temp. (°F)	Test Time (HRS)	Air Flow LITER/HR.	% Viscosity Change	Neut. No. Increase	% Weight Loss	% Oil Insolubles
MLO-7593	700	6	10	———	Solidifies	———	100
MLO-7584	600	20	5	+63	2.2	13	Trace
	700	20	5	+182	3.2	40	0.2
MLO-7582	347	72	5	+5	0.3	2	None
	500	20	5	+67	2.8	8	Trace
	700	6	10	+450	2.3	27	0.3
MLO-7277	347	72	5	+7	0.2	2	0.3
MLO-7583	347	72	5	+69	2.0	1	Trace
	500	20	5	+61	0	0	Trace
MLO-7503	500	48	5	+6	0	1.3	None
	550	48	5	+17	0	1.5	None
MLO-7017	500	20	5	+30	0.7	1.0	Trace

ENCLOSURE 28 AL62T004

LUBRICITY TEST DATA (SHELL 4-BALL WEAR TESTER)

(ALL TESTS UNDER NORMAL ATMOSPHERE USING 1/2" DIAMETER SAE 52100 BALLS)

	Temp. (°F)	Speed (RPM)	Test Time (Hrs.)	Wear Scar Diameter in mm at Loads Indicated		
				5KG	10KG	40KG
MLO-7598	167	620	1	0.26	0.55	0.60
	500	620	1	0.22	0.68	1.38
	600	620	1	0.29	0.97	1.12
MLO-7584	500	620	1	0.21	0.32	1.08
	600	620	1	0.29	0.86	1.69
MLO-7582	167	620	1	0.22	0.47	0.61
MLO-7277	167	620	1	0.11	0.22	0.39
MLO-7451	167	620	1	0.18	0.30	0.46
MLO-7583	167	620	1	0.17	0.28	0.54
MLO-7503	167	620	1	0.31	0.59	0.77
	400	620	1	—	0.80	—
MLO-7017	167	620	1	0.18	0.31	0.67
	500	620	1	0.39	0.77	1.56
	600	620	1	0.34	0.63	1.90

ENCLOSURE 29

AL62T004

SCHEMATIC REPRESENTATION OF EXPERIMENTAL DIRECT BEAM METHODS

FIG.A - VERTICAL SOURCE - PARALLEL PLATES LIMIT VERTICAL DIVERGENCE

FIG.B - HORIZONTAL SOURCE - "POINT SOURCE" GEOMETRY

ENCLOSURE 30

AL62T004

INTENSITY AS A FUNCTION OF SEPARATION

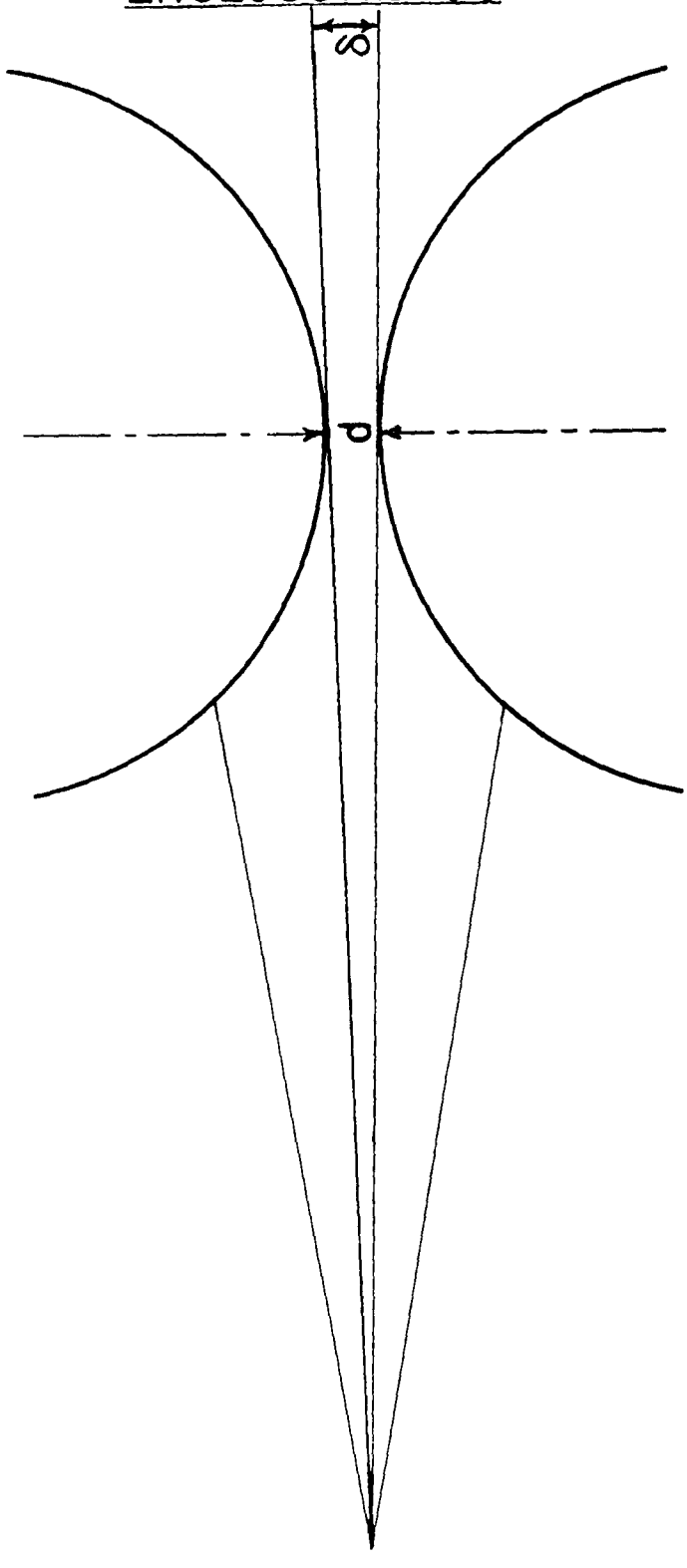

d ≈ δ (IN RADIANS) ∝ INTENSITY

ENCLOSURE 31

AL62T004

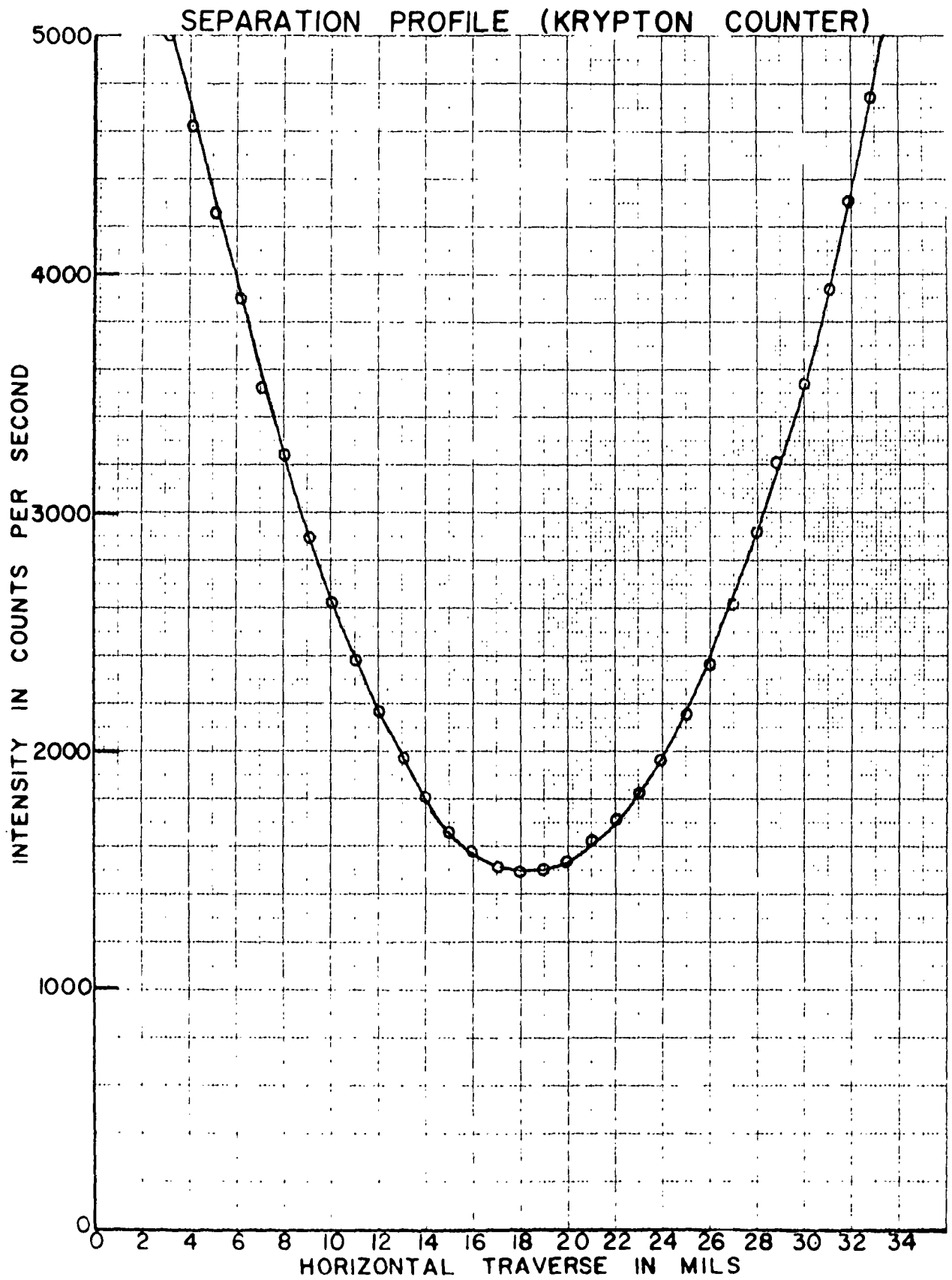

RESEARCH LABORATORY SICF INDUSTRIES, INC.

ENCLOSURE 32

AL62T004

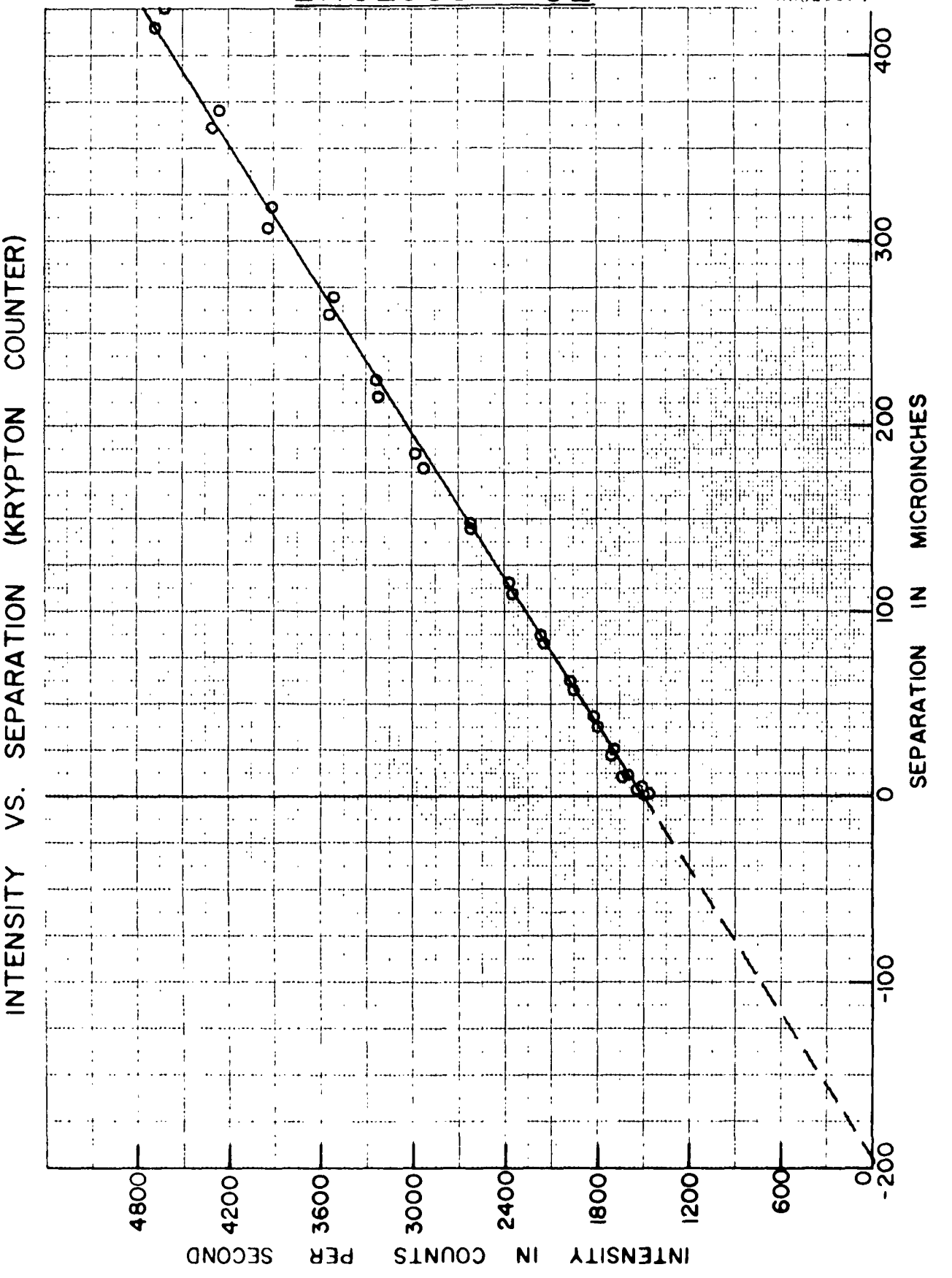

RESEARCH LABORATORY SKF INDUSTRIES, INC.

AL62T004

ENCLOSURE 33

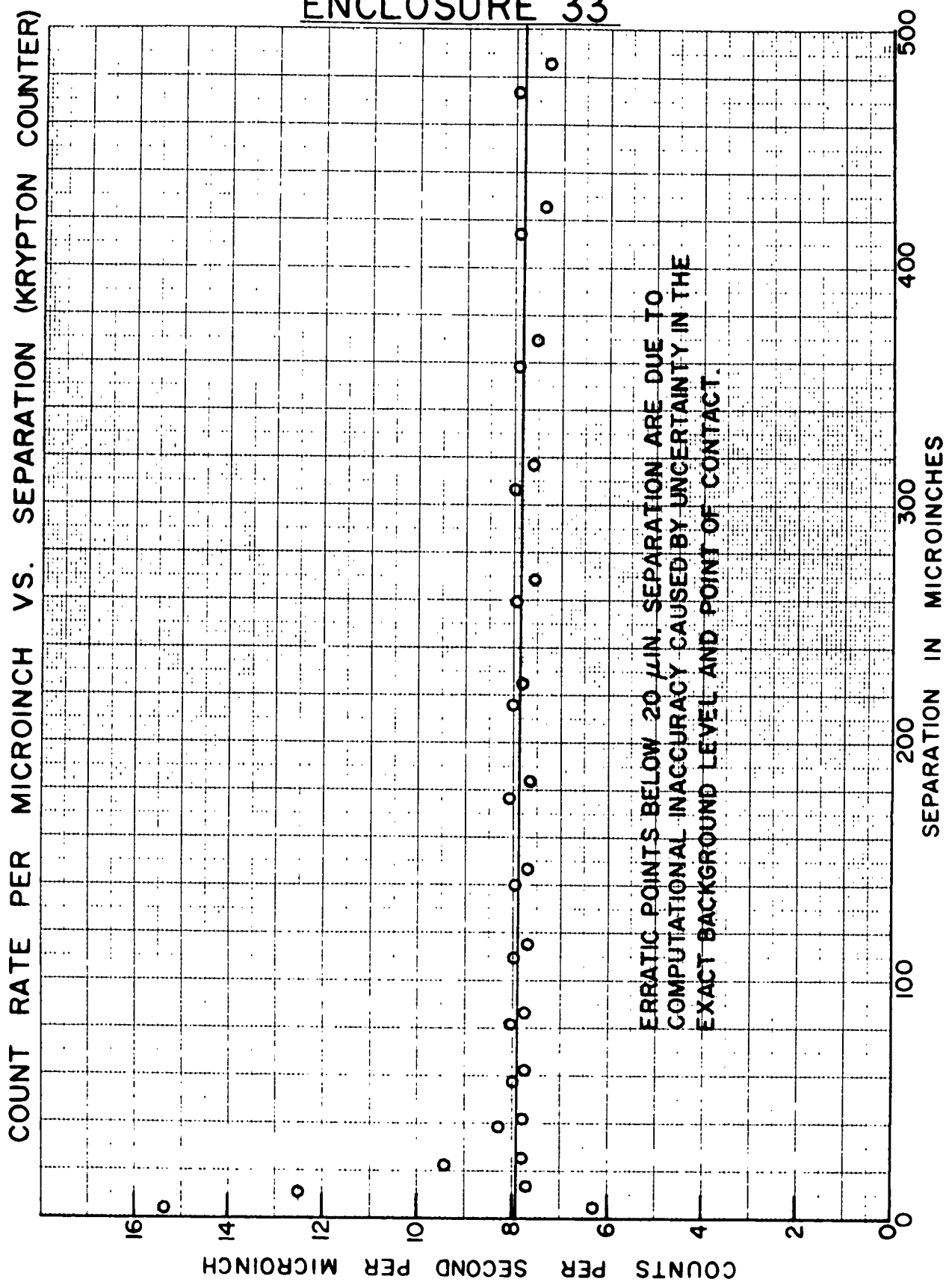

RESEARCH LABORATORY SKF INDUSTRIES, INC.

ENCLOSURE 34

AL62T004

SEPARATION PROFILE (XENON COUNTER)

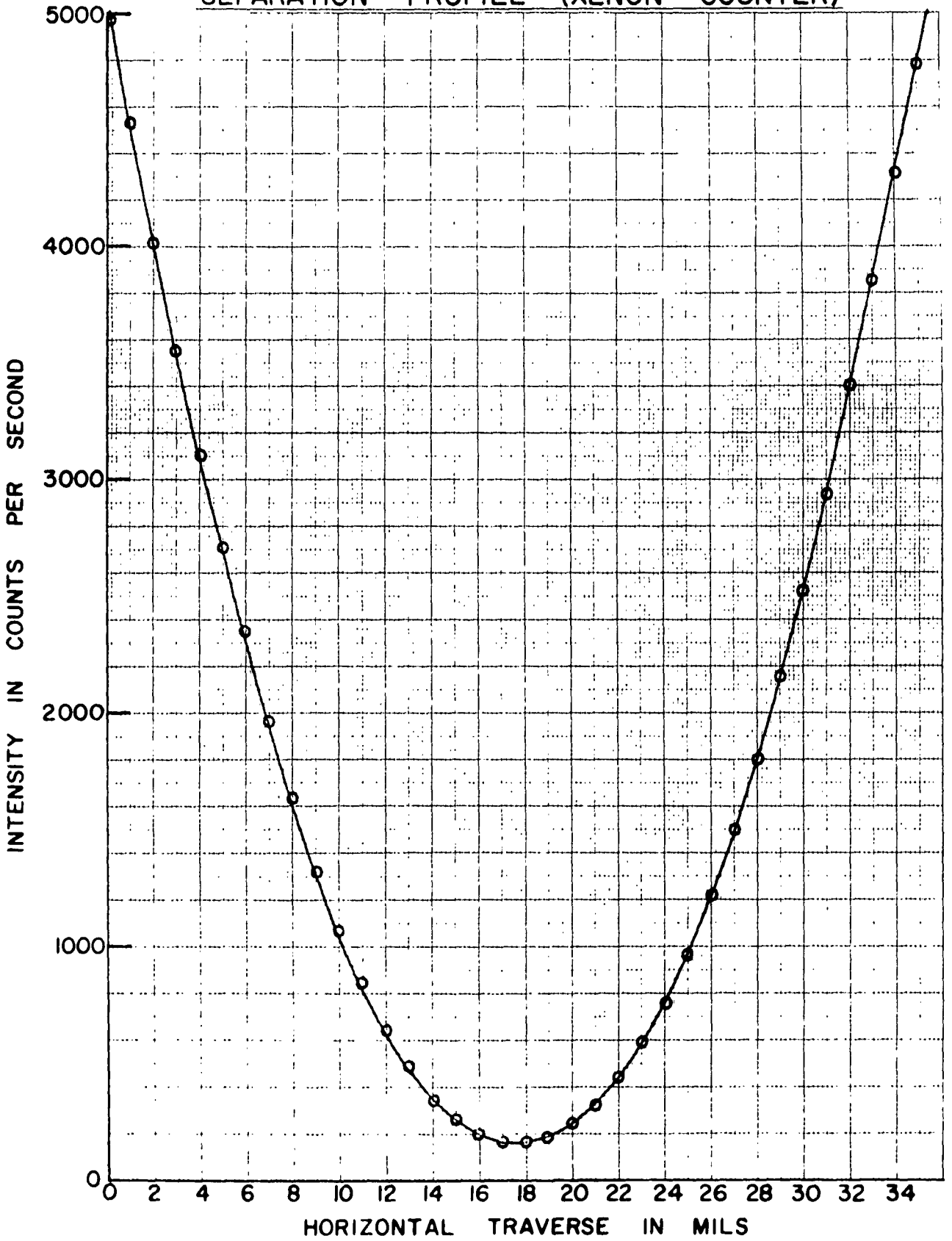

RESEARCH LABORATORY SKF INDUSTRIES, INC.

ENCLOSURE 35

AL62T001

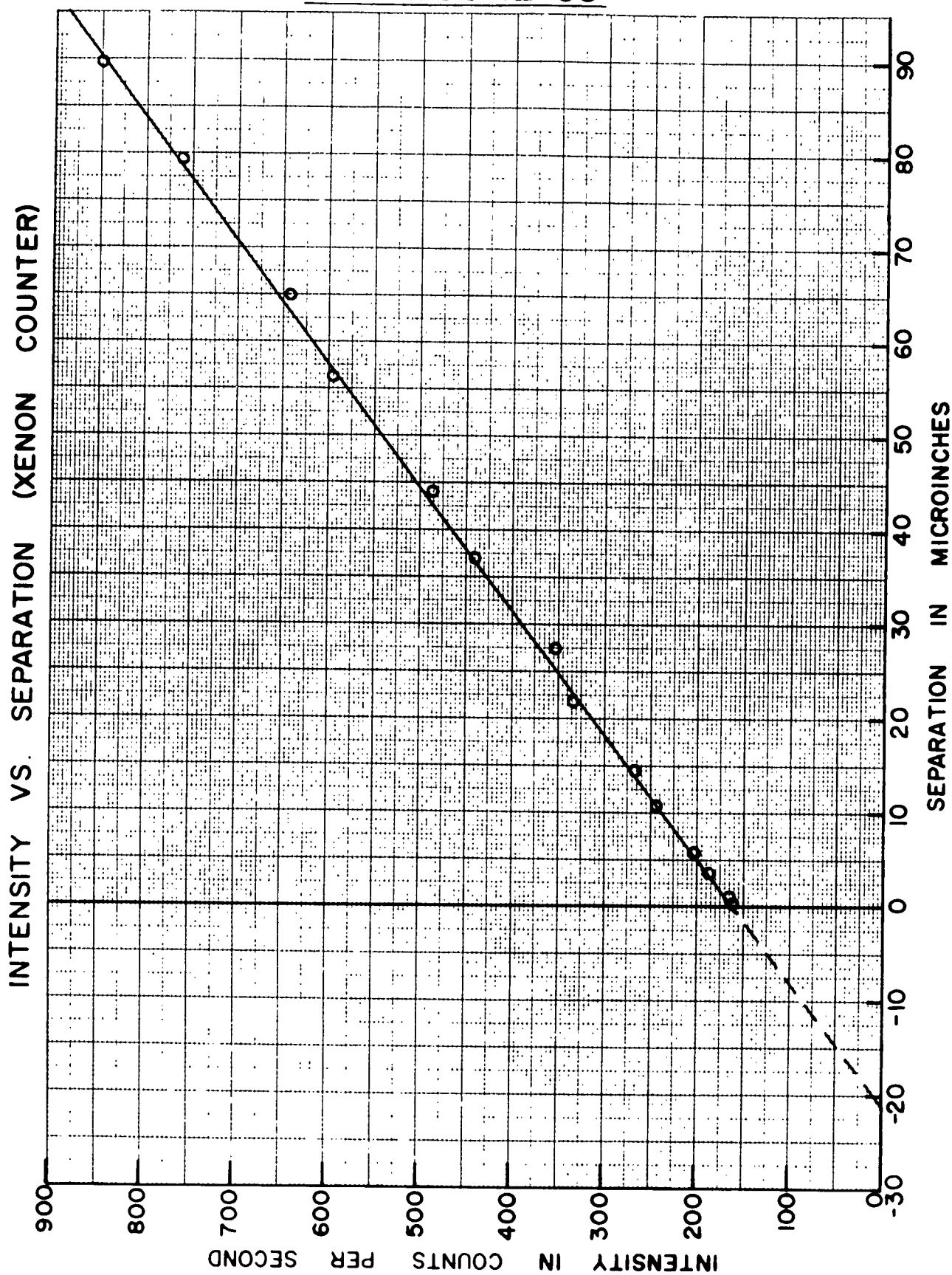

RESEARCH LABORATORY **SKF** INDUSTRIES, INC.

ENCLOSURE 36

AL62T004

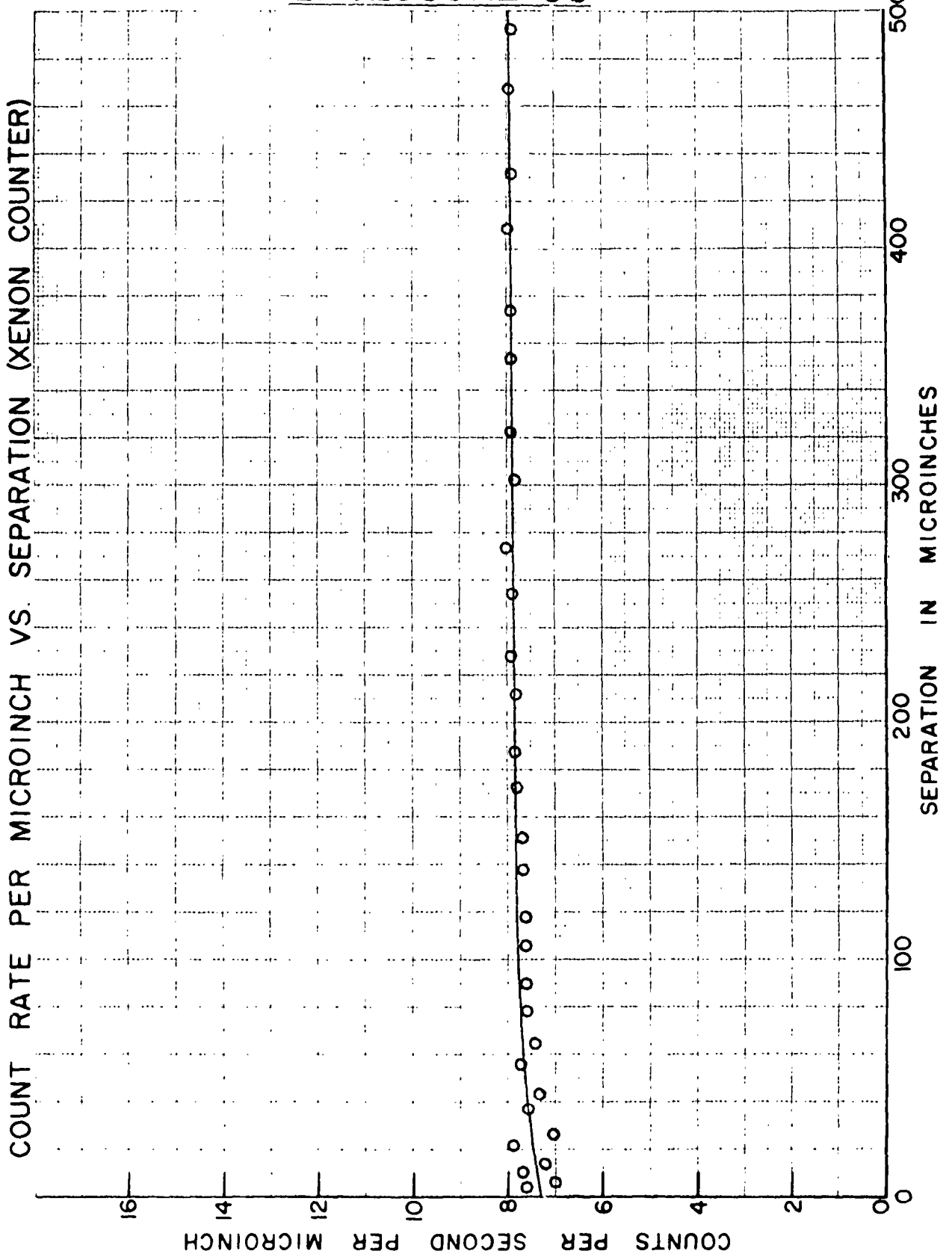

RESEARCH LABORATORY SKF INDUSTRIES, INC.

ENCLOSURE 37

AL62T004

CALCULATION OF PENETRATION ERROR

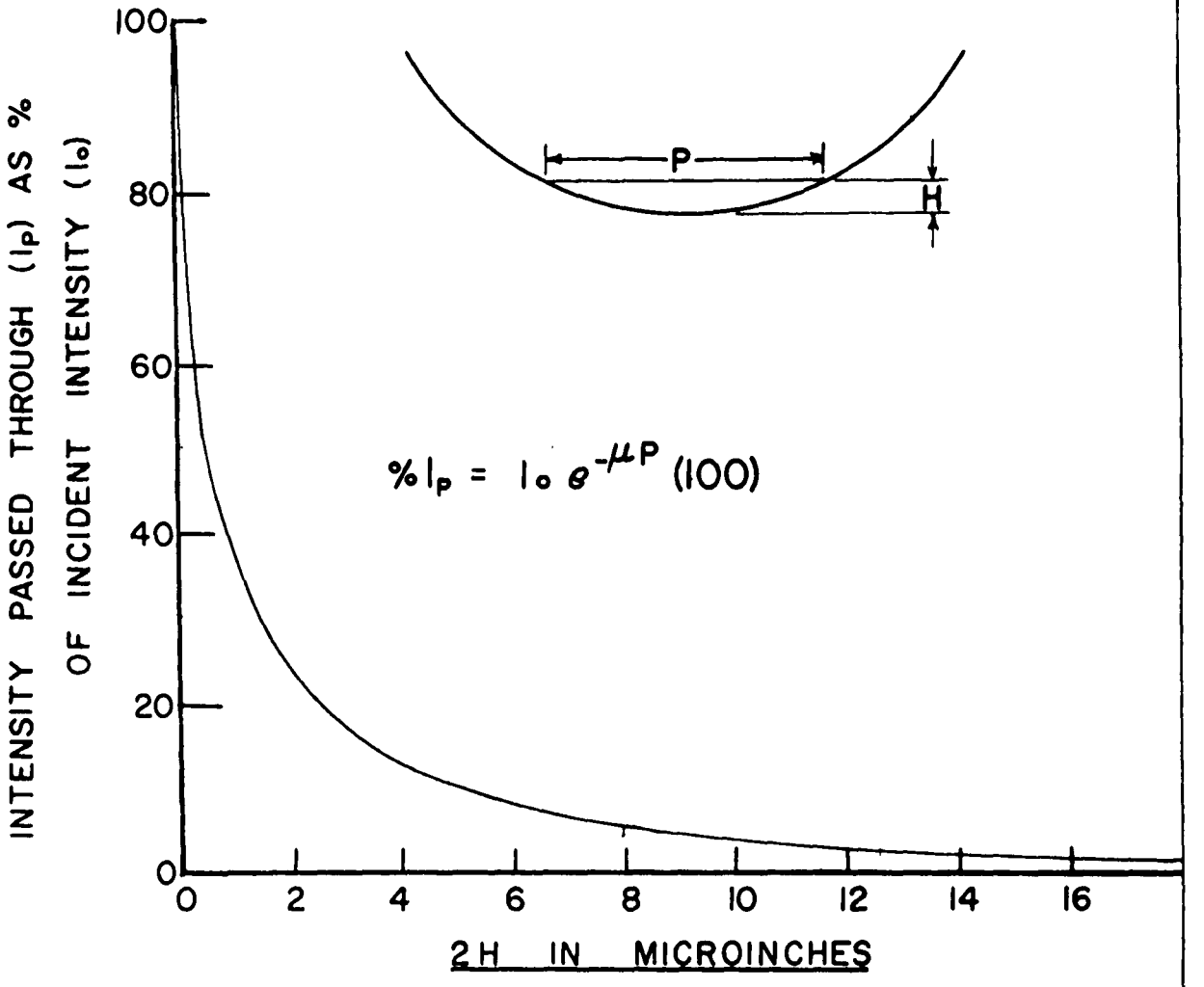

FOR A GIVEN VALUE OF H THE CORRESPONDING PATH LENGTH THROUGH THE BALL IS GIVEN BY;

$$P \approx 2\sqrt{2RH}\ ,\quad 2R = 1''$$

TOTAL INTENSITY PENETRATING BOTH BALLS EQUALS THE AREA UNDER THE CURVE. THIS INTENSITY GIVES AN APPARENT SEPARATION EQUAL TO THE WIDTH OF THE EQUIVALENT RECTANGLE WHOSE HEIGHT IS 100%. THE AREA, MEASURED BY PLANIMETER, GIVES AN EQUIVALENT WIDTH OF 1.8 MICROINCHES.

ENCLOSURE 38

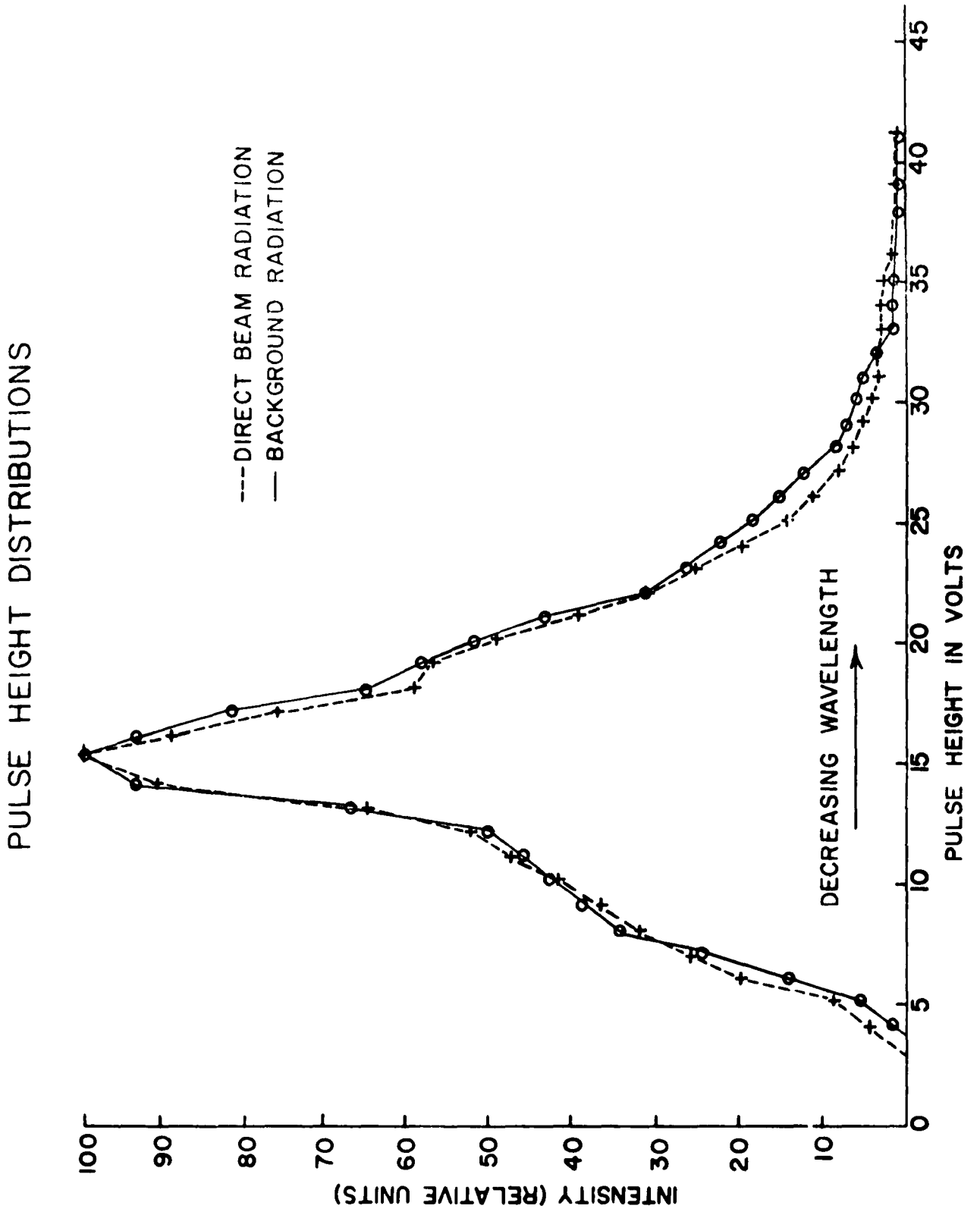

RESEARCH LABORATORY SKF INDUSTRIES, INC.

ENCLOSURE 39

AL62T004

HORIZONTAL DIVERGENCE AND BEAM WIDTH

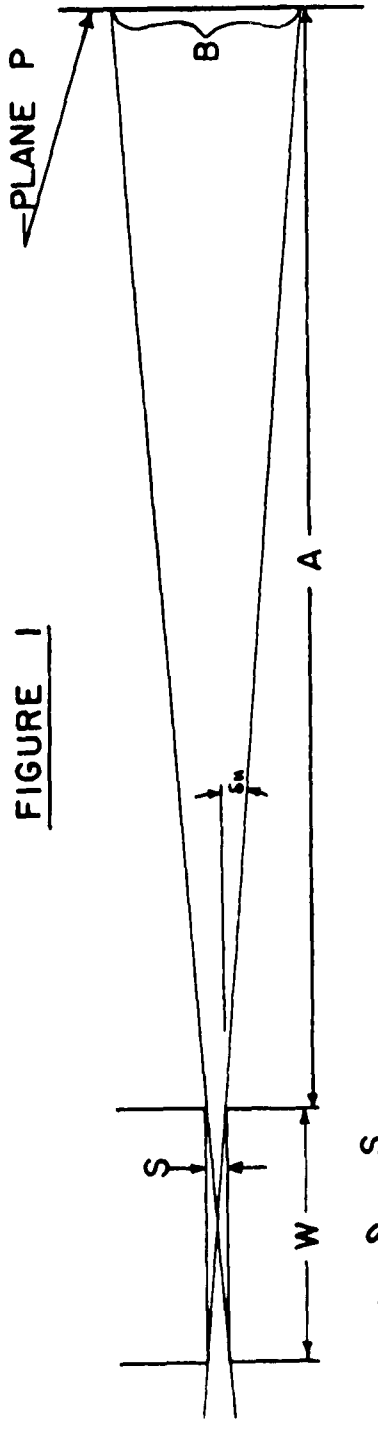

FIGURE 1

$\tan \delta_H = \frac{S}{W}$

$B = S + 2A \tan \delta_H = S + 2A\frac{S}{W}$

THE EFFECT OF SLIT DIMENSIONS AND SLIT TO BALL DISTANCE ON BEAM WIDTH AT THE 2 BALL CONTACT

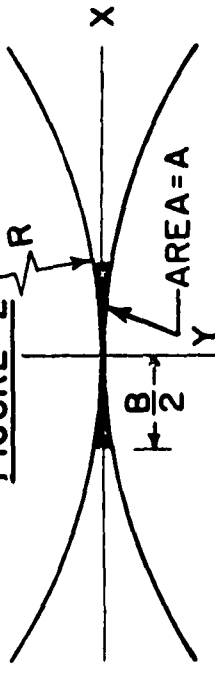

FIGURE 2

RADIUS = R

$$A = 4\int_0^{\frac{B}{2}} \left[R - \sqrt{R^2 - X^2}\right] dX = 4\left[RX\Big|_0^{\frac{B}{2}} - \frac{1}{2}\left\{X\sqrt{R^2 - X^2} + R^2 \sin^{-1}\left(\frac{X}{R}\right)\right\}_0^{\frac{B}{2}}\right]$$

SINCE $B \ll R$, $\sin^{-1}\frac{B}{2R} \approx \frac{B}{2R}$ AND $A = 2RB - RB\sqrt{1-\left(\frac{B}{2R}\right)^2} - 2R^2\frac{B}{2R}$

EXPANDING, $\sqrt{1-\left(\frac{B}{2R}\right)^2} \approx 1 - \frac{1}{2}\left(\frac{B}{2R}\right)^2$, $\therefore A \approx \frac{B^3}{8R}$

BEAM CROSS SECTIONAL AREA, A, AT 0 SEPARATION AS A FUNCTION OF BEAM WIDTH

ENCLOSURE 40

AL62T004

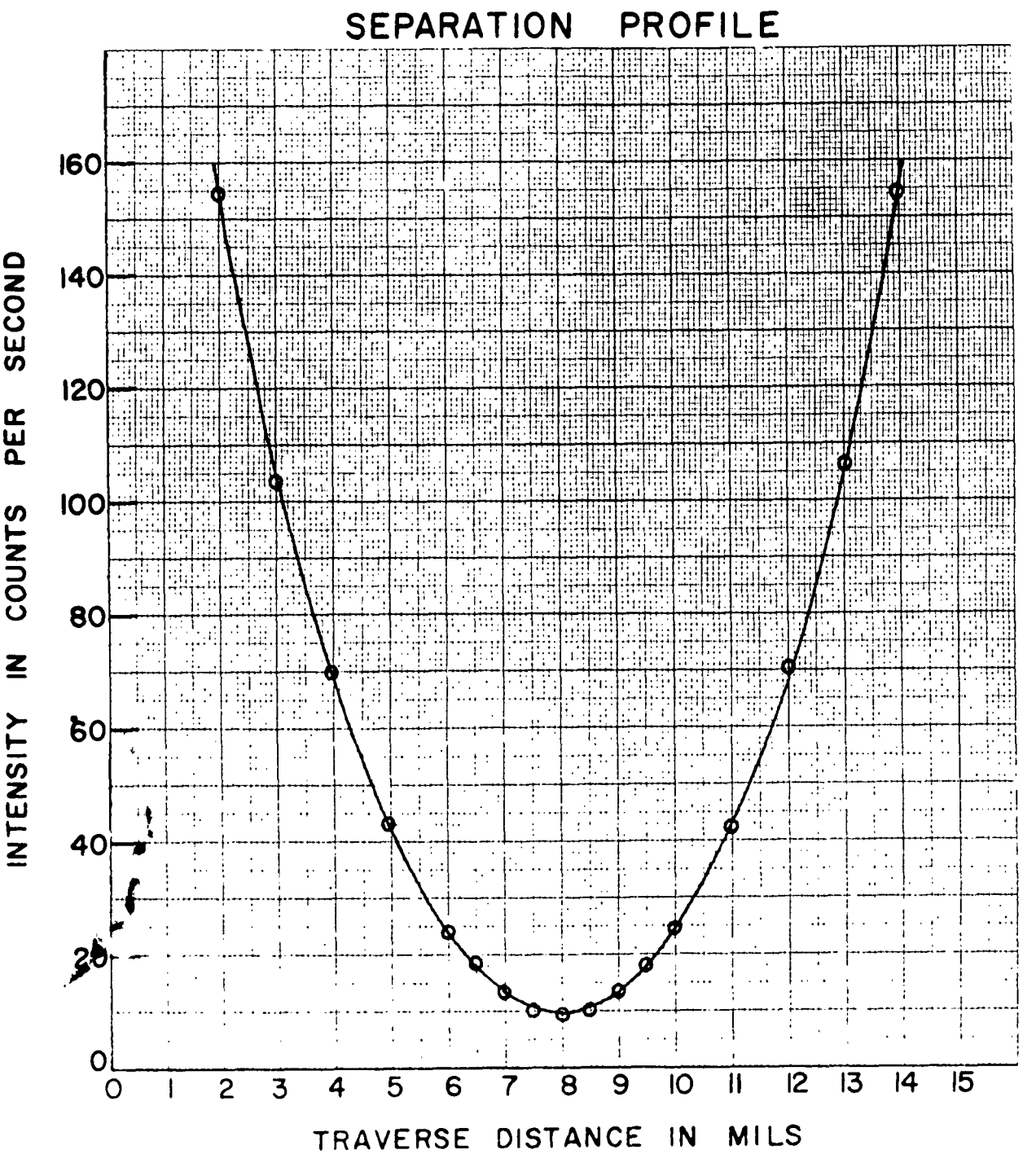

RESEARCH LABORATORY SKF INDUSTRIES, INC.

ENCLOSURE 41

AL62T004

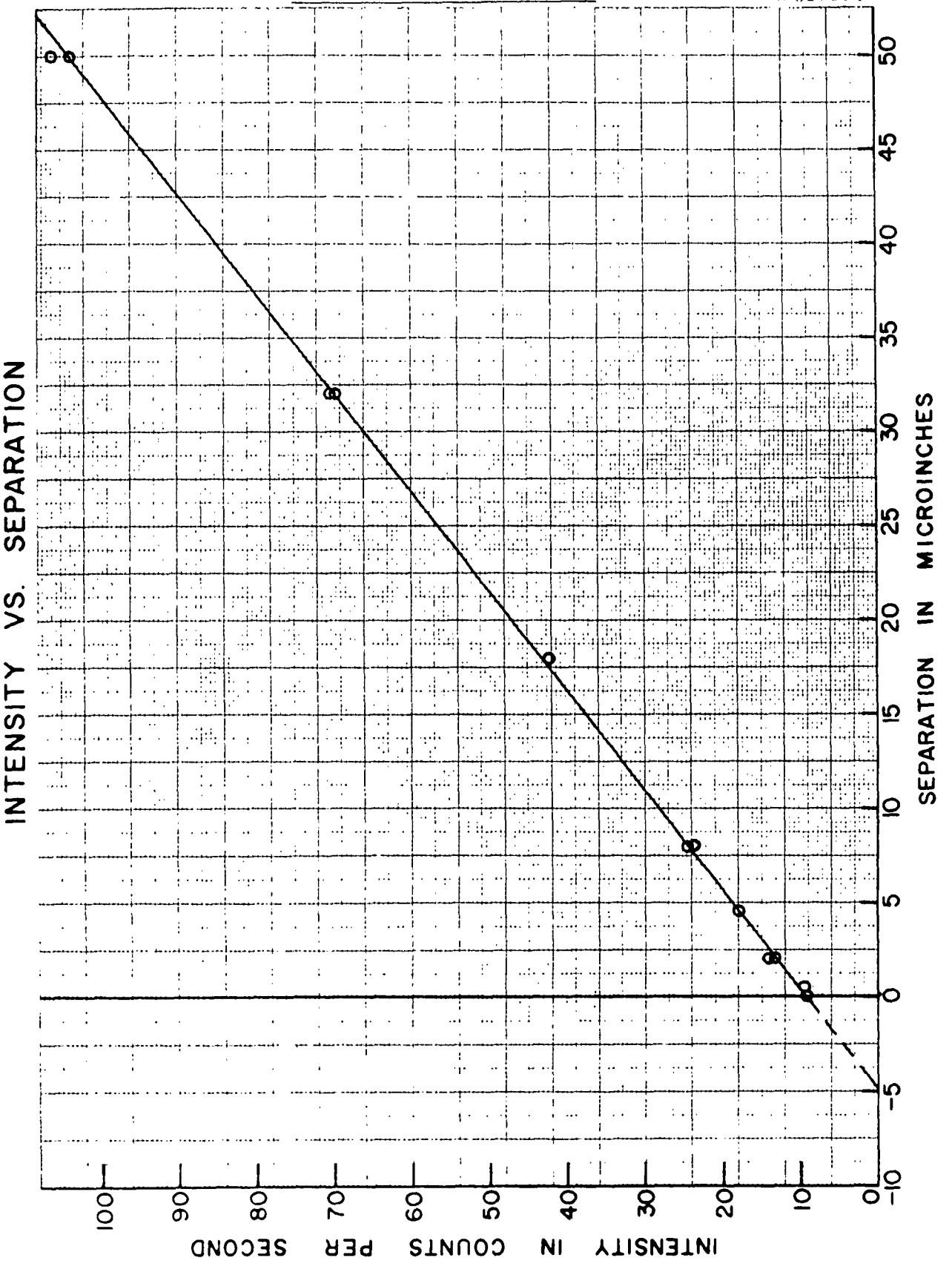

RESEARCH LABORATORY SKF INDUSTRIES, INC.